CO_2 Fluxes Before and After Partial Deforestation of a Central European Spruce Forest

Patrizia Ney[1], Alexander Graf[1], Heye Bogena[1], Bernd Diekkrüger[2], Clemens Drüe[3], Odilia Esser[1], Günther Heinemann[3], Anne Klosterhalfen[1], Katharina Pick[1], Thomas Pütz[1], Marius Schmidt[1], Veronika Valler[4] and Harry Vereecken[1]

Corresponding author: p.ney@fz-juelich.de (P. Ney)

[1]Institute of Bio- and Geosciences (IBG-3): Agrosphere, Forschungszentrum Jülich GmbH, Jülich, Germany

[2]Institute of Geography, University of Bonn, Bonn, Germany

[3]Department of Environmental Meteorology, University of Trier, Trier, Germany

[4]Institute of Geography, University of Bern, Bern, Switzerland

Abstract

A seven year CO_2-flux dataset measured in a 70 year old spruce monoculture is presented, of which 22 % was deforested three years after the start of the measurements to accelerate regeneration towards natural deciduous vegetation. An eddy covariance (EC) system, mounted on top of a tower within the spruce forest, continuously sampled fluxes of momentum, sensible heat, latent heat and CO_2. After clear-cutting, a second EC station with an identical set of instruments was installed inside the deforested area. In total, we examined an EC dataset including three years before (forest) and four years after partial deforestation (forest and deforested). Full time series and annual carbon budgets of the net ecosystem exchange (NEE) and its components gross primary production (GPP) and total ecosystem respiration (R_{eco}) were calculated for both EC sites. Soil respiration was measured with manual chambers on average every month after the deforestation at 75 measurement points in the forest and deforested area. Annual sums of NEE measured above the forest indicated a strong carbon sink of -660 (-535) g C m^{-2} y^{-1} with small interannual variability ±78 (72) g C m^{-2} y^{-1} (values in brackets including correction for self-heating of the open-path gas analyzer). In the first year after partial deforestation, regrowth on the clearcut consisted mainly of grasses, with beginning of the second year shrubs and young trees became increasingly important. The regrowth of vegetation is reflected in the annual sums of NEE, which decreased from a carbon source of 521 (548) g C m^{-2} y^{-1} towards 82 (236) g C m^{-2} y^{-1} over the past four years, due to an increase in the magnitude of GPP from 385 (447) to 892 (1036) g C m^{-2} y^{-1}.

Keywords: Net ecosystem exchange (NEE), Natural succession, Soil respiration, Gross primary production (GPP), Ecosystem respiration, Radiative forcing

1 Introduction

Forest ecosystems in the northern mid-latitudes typically act as a sink for atmospheric carbon dioxide (various authors after Lindauer et al., 2014) and hence play an important role in the global carbon cycle. Disturbances in such ecosystems lead to changes in their carbon balance. Carbon dioxide (CO_2) exchange of a forest ecosystem with the atmosphere is the result of photosynthesis (gross primary production, GPP) and ecosystem respiration (R_{eco}). After a disturbance has occurred, the duration of altered exchange rates depends on the type of disturbance, vegetation species, climate conditions and the post-disturbance land management (Luyssaert et al., 2008; Erb et al., 2018).

Many studies examined forest disturbances like clearcut and stand-replacement (Rannik et al., 2002; Kowalski et al., 2003, 2004; Humphreys et al., 2005; Takagi et al., 2009;

Grant et al., 2010; Aguilos et al., 2014; Paul-Limoges et al., 2015) with different stand ages (chronosequence studies Kolari et al., 2004; Clark et al., 2004; Humphreys et al., 2006; Gough et al., 2007; Amiro et al., 2010; Grant et al., 2010; Paul-Limoges et al., 2015), fire (Dore et al., 2012; Amiro et al., 2006), insect outbreaks (Seidl et al., 2008) and wind-throws (Knohl et al., 2002; Yamanoi et al., 2015; Liu et al., 2016). Some studies focused on Central European forests; e. g., after wind-throw in a mountain forest in the Alps (Matthews et al., 2017), a mixed forest in Sweden (Lindroth et al., 2009) or an upland spruce forest in Germany (Lindauer et al., 2014). Kowalski et al. (2004) examined the effect of harvest on carbon exchange for four different European forest ecosystems by using eddy covariance (EC) measurements and empirical modeling. One main finding of these studies is that the above-mentioned interventions transformed forests from a carbon absorbing to a carbon emitting ecosystem.

The primary purpose of these studies was to determine to what extent an intervention in forest ecosystems changes their carbon balance and influences the global carbon cycle on the larger scale. Crucial questions, among others, are whether the disturbance turns a prior sink becomes a source and if so, when it becomes a sink again, i.e. when the ecosystem carbon compensation point is reached. As a second important, even later point, a payback period can be defined (Aguilos et al., 2014). To date, only few analyses provide an answer to the duration of forest regeneration up to the compensation point based on observation data (Aguilos et al., 2014), because most observations stopped a few years after the intervention (Lindauer et al., 2014; Kowalski et al., 2003, 2004), or including non-continuous time series (Matthews et al., 2017). Information on the payback time could only be provided by studies that used modeled time series (Aguilos et al., 2014) or by assumptions based on chronosequence studies (Noormets et al., 2007; Wang et al., 2014). To our knowledge, there are no studies in which reference measurements in a remaining stand of the same forest ecosystem were collected and evaluated before and after the disturbance.

The study site investigated in this paper is part of the TERENO (Terrestrial Environmental Observatories) network in Germany. The study area consists of a spruce monoculture (originally intended for wood production), which was partially deforested within a re-naturalization project initiated by the management of the Eifel National Park. This opportunity allowed to examine changes in individual ecosystem components and to compare them with the data of a nearby reference area where the spruce forest remained. In recent years, the study area has been intensively examined, particularly with regard to its hydrological (Rosenbaum et al., 2012; Graf et al., 2014; Baatz et al., 2015; Wiekenkamp et al., 2016a,b) and biochemical (Gottselig et al., 2017; Wu et al., 2017) properties.

Here, we compare a seven year EC dataset of the forest, including three years before and four years after the deforestation, and a four year EC dataset from the deforested site (clearcut), to quantify the magnitude of the initial sink-source strength change and the pace of recovery during the first years. In addition to the net ecosystem exchange of CO_2 (NEE) and its data-driven partitioning into GPP and R_{eco}, we consider measured soil respiration (R_s), and compare the climate effect due to changing CO_2 sequestration to the biophysical one due to changed albedo.

2 Material and Methods

2.1 Test site and forest management

The Wüstebach research site, named after the Wüstebach stream and its catchment, is located in the Eifel National Park (50°30'N, 6°19'E) within the Eifel low mountain range in Western Germany and is part of the Lower Rhine Valley / Eifel Observatory in the TERENO network (Zacharias et al., 2011). The catchment covers an area of 38.5 ha (Fig. 1) with an elevation ranging from 595 to 630 m. The slope within the catchment area is 3.6 % on average. Its soils are dominated by Cambisols and Planosols on hill slopes and Gleysols and Histosols in the riparian zone. The main soil texture is silty clay loam with sandstone inclusions (Bogena et al., 2010).

Forestry has dominated the area since the 19th century. Due to a complete deforestation during world war II and reforestation directly thereafter, the predominant vegetation before the clearcut in 2013 was a 70-year-old spruce stock (Norway spruce, *Picea abies L.*) with an area coverage of 90 %. Tree density was 370 trees/ha and tree height 25 m on average (Etmann, 2009). Small parts in the northern part of the study area, particularly along the Wüstebach stream, were covered with meadow (6 %) and the central part of the catchment was covered by peat bog and half-bog with an alder stock near the stream (Lehmkuhl et al., 2010). By using allometric biomass functions, a dry biomass of about 310.5 t ha^{-1} was calculated for the forest area two years before CO_2 flux measurements started, including above and below ground living biomass and deadwood (8.1 t ha^{-1}, Etmann, 2009).

Information about the leaf area index was collected with a SunScan-System SS1 (Delta-T devices, Cambridge, UK) from April 2016 until July 2017 at least once per month in the clearcut and during five dates in the forest in a plot of 10 different locations for the clearcut and 60 for the forest. The mean LAI between the years 2016 and 2017 was 4.2 ($\pm$0.3) and 2.0 ($\pm$0.4) in the forested and deforested area, respectively.

Since 2007, the Wüstebach site has been instrumented with a large variety of measurement equipment to obtain information about hydrological, chemical and meteorological states and fluxes (Bogena et al., 2015). In 2010, a 37.8 m high tower was erected, which hosts an EC station and meteorological measurements.

In September 2013, 8.6 ha of the spruce monoculture forest was deforested. The clearcut area is located in the north-east part of the catchment and was allowed to regenerate naturally towards near natural mixed beech forest. A cut-to-length logging method was applied, where only 3 % of the original biomass was left on-site (Baatz et al., 2015). In the first year after deforestation, the area grew mainly with grasses (e.g.: *Deschampsia flexuosa (L.) Trin.*, *Luzula luzuloides (Lam) Dandy & Wilmott* , *Galium saxatile L.*), red foxglove (*Digitalis purpurea L.*) and fireweed (*Epilobium angustifolium (L.) Holub*). In the following years, new trees appeared, among them in large parts rowan (*Sorbus aucuparia L.*), but also spruce (*Picea abies L.*), birch (*Betula L.*), aspen (*Populus tremula*

L.) and elder (*Sambucus L.*). Shrub vegetation spread extensively and comprised broom (*Cytisus scoparius (L.) Link*), heather *(Calluna vulgaris (L.) Hull)* and European blueberry *(Vaccinium myrtillus L.*). Bulrushes (*Juncus effusus L.*) grew in the wet areas mainly at the edge of the stream.

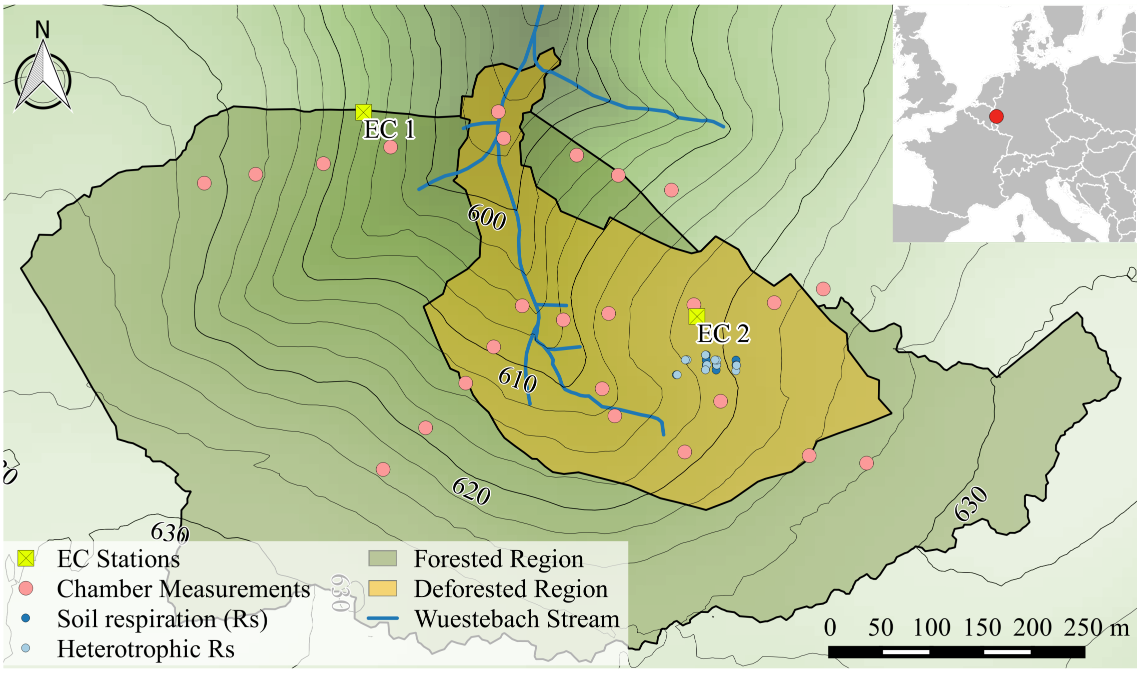

Figure 1: Overview of the study area Wüstebach and locations of the measurements after partial deforestation in September 2013. Chamber measurements marked by blue colored dots were performed before deforestation in order to obtain information about the heterotrophic and autotrophic proportion of soil respiration (R_s).

2.2 Eddy covariance measurements and quality control

Turbulent fluxes of CO_2 (F_{CO_2}), water vapor (λE) and sensible heat (H) were measured by two continuously operating EC stations in the forested area since June 2010 and in the deforested area since September 2013. Both stations comprised a three-dimensional sonic anemometer (CSAT-3, Campbell Scientific, Inc., Logan, Utah, USA) and an open-path infrared gas analyzer (IRGA, LI-7500, Li-Cor, Inc., Biosciences, Lincoln, Nebraska, USA), whereby the latter were installed with an inclination of 45°. The sensor separation between the sonic anemometer and the IRGA was 0.15 m for the forest EC station and 0.22 m for the clearcut EC station. Both analyzers were calibrated every three months. The forest EC system was mounted on top of a tower at 37.8 m a.g.l., located in the western part of the forested catchment. The second EC station was placed in the deforested area. Its measuring height of initially 2.5 m a.g.l. was changed in June 2017 to 3 m due to vegetation growth. The measurement frequency for both stations was 20 Hz. Turbulent fluxes were calculated as 30-min averages using the TK3.11 software package, which includes rigorous correction procedures and quality control (Mauder and Foken, 2011; Mauder et al., 2013). Additional to the WPL density-flux correction (Webb (1982), implemented in TK3.11) we also considered the correction for self-heating of open-path IRGA after Burba et al. (2008), using site-specific non-gap-filled meteorological data. Since correction terms in Burba et al. (2008) are generally performed for vertically adjusted sensors and our analyzers were mounted inclined to reduce the influence of self-induced heat fluxes, we used a modified form of the correction with a scaling parameter to account only a fraction of the additional heat flux (Järvi et al., 2009; Kittler et al., 2017). Since there is no general consensus on the application of the correction, we decide to show both variants of the resulting CO_2 fluxes, the uncorrected and the self-heating corrected. The corrected flux was calculated considering a scaling factor to reduce the fraction of the additional heat flux for sensors installed with inclination (as described above). The scaling factor used in the literature was determined for an inclination of 15°, much less than at our case. Consequently, we assume that the corrected data indicate the values for the most unfavorable case and that real CO_2 fluxes lie between these and the values without correction. For clarity, the following figures and calculations are based on the uncorrected fluxes, only for the cumulated fluxes both variants are given, whereby the corrected quantities are denoted with the suffix 'CB' (correction after Burba et al. (2008)) and values within the text are given in brackets. As a result of the TK3.11 processing, flux data were assigned to three quality classes (good, moderate, bad). For this study, data of good and moderate quality were used.

For measurements above tall canopies, NEE is composed of F_{CO_2} and the CO_2 storage flux (F_s) in the air column below the EC measurement height. However, CO_2 profile measurements were not existing at the study site and F_s was estimated from a single point CO_2 measurement as suggested by Hollinger et al. (2004).

In the first six months of the measuring period, no internal diagnostic flag of the IRGA was logged, which is essential for qualitiy checking prior to flux calculations. Therefore, a subsequent quality check was performed by comparing the absolute humidity measured with the IRGA against the absolute humidity calculated from on-site low frequency measurements. Measured IRGA values were excluded if the absolute humidity differed more than 2 g m^{-3}.

An additional method to check the plausibility of the EC measurements is the comparison between measured turbulent fluxes and the available energy (e. g., Wilson et al., 2002). The energy balance equation is:

$$Q - B = H + \lambda E + Res \qquad (1)$$

where Q is net radiation, B is ground heat flux (the storage term of soil heat flux SHF was calculated according to Campbell Scientific (2003) and added to measured SHF), H and λE are eddy covariance fluxes for sensible and latent heat, respectively. Res includes all fluxes, which are not detected by the EC stations (i.e. advection terms, canopy heat storage and others). The energy balance closure (EBC) was estimated using a linear regression between the available energy (Q–B) and the energy fluxes (H+λE). Additional, the energy balance ratio (EBR) was calculated as the sum of the turbulent fluxes divided by the available energy (Wilson et al., 2002). The residual term Res considered the heat storage of the vegetation and the heat storage caused by temperature and latent heat changes in the canopy air. The storage terms were calculated according the procedure and equations given in Moderow et al. (2009). The canopy heat storage between the ground and the measuring height was determined from the temperature profile (six levels) at the forest tower. The storage change of latent heat in the canopy air was calculated using the humidity measured from the gas analyzer. Biomass temperature was assumed to be equal to the mean surface temperature of the stems. Wet biomass was estimated as 37.7 kg m^{-2} (2009, Etmann, 2009). For canopy specific heat capacity a value of 2.958 J kg^{-1} K^{-1} was used (Moderow et al., 2009). Due to numerous and large gaps in the data basis of the auxiliary meteorological measurements (temperature profile, trunk space temperature and Q), the EBC of the forest EC station was determined only for the year 2013. *Res* was neglected for the clearcut EC station.

The footprint of the observed F_{CO_2} was determined using an analytical footprint model included in the software package TK.311, which was developed according to Kormann and Meixner (2001). We evaluated the cumulative footprint every 30 min for the forest and clearcut EC station up to a distance of 3 km and 1 km, respectively. Target areas were set to calculate the flux contribution originating from the area of interest. Subsequently, all 30-min NEE fluxes with less than 70 % contribution from the target area (i.e., spruce forest and deforested area, respectively) were rejected.

2.3 Measurements of meteorological parameters

The meteorological tower at the forest site is equipped with a net radiometer (NR01, Hukseflux Thermal Sensors, Delft, Netherlands) and a photosynthetically active radiation (*PAR*) quantum sensor (SKP 215, Skye Instruments Ltd, Llandrindod Wells, UK), which were installed on a 5 m long extension arm at 34 m a.g.l.. Relative humidity and air temperature (HMP45, Vaisala Inc., Helsinki, Finland) were measured at 38 m a.g.l.. Additional, air temperature was measured at levels of 38, 31, 27, 24, 16 and 8 m by ventilated and radiation shielded PT-1000 (CS240, Campbell Scientific, Inc., Logan, Utah, USA). Three infrared remote temperature sensors (IR120, Campbell Scientific, Inc., Logan, Utah, USA) were mounted 2 m a.g.l. and sampled surface temperatures of the soil surface, undergrowth and trunk space. In the immediate vicinity of the tower, the soil temperature T_s (thermistor type 107, Campbell Scientific, Inc., Logan, Utah, USA) and soil water content SWC (CS616, same manufacturer) were measured with three sensors each at 0.02, 0.05, 0.1, 0.2, 0.5 and 0.8 m depth. Three heat flux plates (HFP01, Hukseflux Thermal Sensors, Delft, Netherlands) measured the SHF at 0.05 m depth. All micrometeorological parameters were sampled continuously in 10-min intervals.

The EC station at the deforested area was additionally equipped with sensors for air temperature and relative humidity (HMP45C, Vaisala Inc., Helsinki, Finland), radiation quantities (NR01, Hukseflux Thermal Sensors, Delft, Netherlands) and PAR (Li190, LI-COR, Lincoln, Nebraska, USA). Precipitation P (pluviometer Pluvio^2, OTT Hydromet, Kempten, Germany) was sampled at a separate weather station close to the EC station. Furthermore, SHF was measured using three soil heat flux plates (HFP01, Hukseflux Thermal Sensors, Delft, Netherlands), two deployed in a depth of 0.02 m and one in 0.08 m. T_s (0.01, 0.04 and 0.05 m) and SWC (0.025 m) were measured using thermocouple probes (TCAV, Campbell Scientific, Inc., Logan, Utah, USA) and two water reflectometers (CS616, same manufacturer).

Meteorological parameters which were not available at the Wüstebach site but used in this work for gap-filling came from the TERENO research site Schöneseiffen (50°30'N, 6°22'E, 610 m a.s.l., multi-sensor WXT510, Vaisala Inc, Helsinki, Finland). This station is located about 3 km northeast on an open meadow area.

2.4 Chamber measurements

Soil respiration (R_s) measurements with two portable chambers (survey system LI-8100, Li-Cor Inc., Lincoln, Nebraska, USA) started in October 2013, shortly after the clear-cutting. Three polyvinyl chloride (PVC) collars were installed at each of 25 measuring locations (75 measurements in total), which were arranged in transects through the forest (twelve locations) and clearcut (thirteen locations, Fig. 1). The collars had a diameter of 0.2 m and a height of 0.07 m and were installed such that they protruded 0.02 m above the soil surface. They were left in place during the entire measurement period with occasional re-fitting, if required. Vegetation inside the collars was not removed completely, as it would have affected the soil structure, but kept short by clipping preferably after measurements. On measurement days with a partial or complete snow cover (December 2014, January, March and November 2015, January and November 2016), the columns were carefully cleared from the snow prior to the measurement where necessary. The chamber was placed once on each collar and CO_2 as well as water vapor concentration and chamber headspace temperature were logged every second. The chamber was closed for 90 sec in total, while only the last 60 sec were used for flux calculation by fitting a linear regression to CO_2 concentrations. Fluxes were subsequently corrected for changes in air density and water vapor dilution. Chamber measurements were performed monthly at the same time of the day around noon. Between January and September 2016, measurements were taken every two months.

To investigate the relationship between R_s and T_s at the deforested area, T_s data measured at the clearcut EC station were used with the corresponding monthly R_s measured in immediate vicinity to the station (approx. 3 m distance). T_s was selected from a 10-min dataset such that it was closest to the time of the chamber measurement of the second soil collar of the triple. R_s was averaged over all three measured collars. In the next step, we fitted the observed data to an empirical exponential van 't Hoff type equation (van 't Hoff, 1989; Lloyd and Taylor, 1994):

$$R_s = a \cdot exp^{(bT_s)}, \tag{2}$$

where a and b are regression coefficients. The parameters a and b were used to calculate the base respiration R_{sb10} at 10°C:

$$R_{sb10} = exp^{(a10+b)}, \tag{3}$$

and the Q_{10} relationship which describes the temperature sensitivity of R_s:

$$Q_{10} = exp^{(10b)}. \tag{4}$$

For calculating the R_s/R_{eco} fraction, a mean was computed for all measured transect R_s values (36 in the forest and 39 in the deforested area) for every measurement day. Half-hourly R_{eco}, calculated after Lasslop et al. (2010) (see Section 2.5), were paired with corresponding R_s measurements to calculate a ratio.

In order to obtain information regarding the proportion of heterotrophic and autotrophic respiration to R_s, an additional dataset (April 2011 to March 2014) was evaluated. The installation of the measurement grid is described in Dwersteg (2012) and comprised eleven measuring points with root exclusion, two of which were treated with the method of root elimination, and nine with the method of root trenching. Steel (for trenching) and plastic collars were used with the usual diameter of 0.2 m, but a a length of 0.4 m to avoid re-invasion by roots. The grid was located about 150 m south of the clearcut EC station inside the spruce forest before deforestation. Here, R_s was measured on a weekly basis with the same chamber system and procedure as described above. Autotrophic respiration was calculated by subtracting measured heterotrophic respiration (measurement points with root exclusion) from R_s measured at the corresponding control points.

In an effort to prepare future long-term measurements and to test the relevance of a possible confounding effect of manual measurements at a fixed daytime (Keane and Ineson, 2017) for our site, we installed one automated chamber near the forest and one near the clearcut EC station in May 2017 (for more information see Appendix). The system (Li-8100, Li-Cor Inc. Biosciences, Lincoln, Nebraska, USA), collar size, closure time and analysis strategy were the same as with the manual measurements, while the closure interval was 30 min. Results of these measurements are shown in the Appendix.

On the same day when the monthly R_s measurement were carried out, a transparent chamber was operated inside the cleacut area to sample daytime values of NEE and evapotranspiration. The minimum disturbance chamber has a rectangular tunnel shape with a surface area of 1.6 m^2 and is passively ventilated through the in- and outlet of the tunnel. Due to the passive ventilation principle of the system, measurements had to be excluded when the wind was weak or the wind direction changed within one measuring day. A detailed description of the system and the validation against EC measurements in homogeneous ecosystems is given in Graf et al. (2013). The location of the chamber was changed frequently within the clearcut area and included grass locations as well as bog vegetation. In the context of this study, we focus on these chamber measurements as an additional check on the magnitude of EC fluxes measured on the clearcut (Sect. 3.2).

2.5 Gap-filling and source partitioning

Data gaps in meteorological variables of air temperature, humidity and global radiation ($S\downarrow$) were filled with a variant of the data interpolating empirical orthogonal functions (DINEOF) method (Beckers and Rixen, 2003; Graf, 2017), using linear relations to the same variables measured by up to 19 other TERENO stations in a radius of 50 km.

The R package REddyProc (REddyProc Team, 2014), which follows mostly the standardized FLUXNET gap-filling procedure, was used to fill gaps in half-hourly EC data. This method uses marginal distribution sampling or look-up table similar to Falge et al. (2001) with additional consideration of co-variation of fluxes with meteorological variables and temporal auto-correlation of fluxes described in Reichstein et al. (2005).

Before gap-filling, friction velocity (u_*) filtering was applied to remove NEE data measured under conditions with insufficient turbulence. To identify the u_*-threshold we used a change point detection method described in Barr et al. (2013) (implemented in REddyProc) and was applied to annual subsets of the data. For the forest and clearcut EC stations, thresholds were estimated by 0.35±0.05 m s^{-1} and 0.13±0.01 m s^{-1}, respectively.

The most common method to disentangle GPP and R_{eco} from directly measured NEE is the nonlinear regression method (NLR) based on parameterized non-linear functions, which express semi-empirical relationships between net ecosystem flux and environmental variables, commonly temperature and $S\downarrow$. Many different versions have been implemented (Falge et al., 2001; Hollinger et al., 2004; Barr et al., 2004; Desai et al., 2005; Richardson and Hollinger, 2007; Noormets et al., 2007). Here, we used a daytime data-based flux-partitioning algorithm after Lasslop et al. (2010), implemented in REddyProc.

NEE was modeled using a rectangular hyperbolic light-response curve, taking into account the temperature dependency of respiration and vapor pressure deficit limitation of photosynthesis.

To avoid discontinuities and minimize extrapolation, the datasets were not generally split into e.g. annual subsets before gap-filling and source partitioning. However, the forest dataset had to be split in the center of one particularly long data gap, which occurred from mid-December 2016 to early March 2017.

2.6 Assessment of albedo effect

Afforestation and deforestation affect local and global climate through a multitude of pathways. Beside the net CO_2 exchange, which typically dominates the biogeochemical feedback, changed albedo (α) is often considered an important factor. This biophysical effect can override biogeochemical ones (Betts, 2000), especially during the first years after a land use change, because its radiative forcing is immediate as opposed to the slow, continuous accumulation of forcing by a CO_2 source or sink. If the effects of α and NEE are opposite and steady in time, these different temporal dynamics of both result in a compensation time after which the cumulating CO_2 forcing overrides the steady albedo forcing again. According to Rotenberg and Yakir (2010) the compensation time can be on the order of tens of years.

On the temporal scale of our study, the short-term dynamics of both NEE and α on the clearcut cannot be ignored, and estimation of a compensation time from both changing quantities might be premature. We used the same basic equations as Rotenberg and Yakir (2010), but rather than solving for compensation time, we explicitly computed radiative forcing of both the (instantaneous) albedo effect and (cumulative) NEE effect for the end of each year after clear-cutting. The global increase in atmospheric CO_2 dry mole fraction due to a local sink or source is

$$\Delta\chi_{CO2} = \frac{\beta \cdot NEE \cdot t \cdot A_{site} \cdot M_a}{m_a \cdot M_c} \tag{5}$$

(compare Betts, 2000), where t is time, A_{site} is the surface area of the ecosystem, m_a is the mass of the atmosphere (5.15·10^{21} g), M_a and M_c are the molar masses of air and carbon required if NEE is given in g C per area and time ($M_a/M_c = 2.414$), and β is an estimate of the airborne fraction (0.5). The resulting radiative forcing

$$RF_{NEE} = 5.35 \cdot \ln(1 + \frac{\Delta\chi_{CO2}}{\chi_{0,CO2}}) \tag{6}$$

(Myhre et al., 1998), where 5.35 is an empirical value in W m^{-2} and $\chi_{0,CO2}$ is the base concentration to which the change is applied (~ 400 ppm in our case), can be linearized for $\Delta\chi_{CO2} \ll \chi_{0,CO2}$ to yield $RF_{NEE} \approx 5.35 \cdot \Delta\chi_{CO2}\,\chi_{0,CO2}^{-1}$. The global radiative forcing of a local surface albedo change, neglecting any net side effect on the long-wave radiation budget, is

$$\Delta RF_\alpha = \overline{S\downarrow} \cdot \Delta\alpha \frac{A_{site}}{A_E}, \tag{7}$$

where $\overline{S\downarrow}$ is the mean incoming short-wave radiation, $\Delta\alpha$ is the difference in albedo between two land surfaces or between before and after change, and A_E is the surface area of the earth (5.1·10^{14} m^2). Here, we used only high-quality local measurements of radiation at each of both sites (Sect. 2.3) to determine its α as the ratio between the annual sums of jointly available outgoing and incoming shortwave radiation values. To remove any effect of small interannual fluctuations of annual $S\downarrow$ on the analysis, and accommodate longer data gaps in forest tower radiation, we used for all four years after the deforestation a constant $S\downarrow$ computed as the average of the gap-filled (Sect. 2.5) $S\downarrow$ at the clearcut site over the whole period, and a constant forest α based on the study year 2013-2014. The clearcut α, in contrast, was updated for each study year to accommodate for changes resulting from vegetation regrowth. Due to the linearization of RF_{NEE} we can drop A_{site} from both equations 5 and 7 (thus reporting the global effect of each square meter of treated land surface), compute ΔRF_{NEE} between both surfaces directly as a function of their NEE difference ΔNEE, and cumulate it over years. Hence, the combined radiative forcing ($\sum_{RF}$) from both NEE and α is

$$\sum_{RF} = \frac{RF_y}{A_{site}} = \frac{\overline{S\downarrow} \cdot \Delta\alpha_y}{A_E} + \sum_{i=1}^{y} \frac{5.35\,W\,m^{-2} \cdot \beta \cdot \Delta NEE_i \cdot M_a}{\chi_{0,CO2} \cdot m_a \cdot M_c}, \tag{8}$$

where the indices y and i indicate the study year (year after deforestation) under consideration. It has already been clarified by Rotenberg and Yakir (2010) that such a radiative forcing-based comparison is only a rough, convenient way to compare the magnitude of the two presumably most important, often opposite warming and cooling effects of land use change. In the context of our study it is used to demonstrate how CO_2 budget changes, which remain the focus of this paper, can be offset by biogeophysical effects.

3 Results and Discussion

3.1 Meteorological conditions during the observation period

The climate at the study site is influenced by the Atlantic Ocean with relatively high rainfall. The long-term mean annual temperature is 7°C and the mean annual precipitation is 1332 mm (reference period 1981-2010, temperature data are taken from the DWD station Schneifelforsthaus and precipitation from Kalterherberg). Winters are moderately cold with periods of snow. Annual average snow duration (snow coverage $\geq$ 50 %) was 50 days with a mean snow depth of 13 cm (1981-2010). Summers are often characterized by relatively humid and cool conditions. The prevailing wind direction is south-west. Figure 2 shows the meteorological conditions from 1 January 2011 until 30 September 2017. Within the considered time-frame, annual mean air temperature (T) at the research site ranged between 7.1°C (year 2013) and 8.9°C (year 2014) with an annual average of 8.2°C for the entire measurement period (Tab. 1). Annual sums of P ranged between 990 mm (year 2013) and 1358 mm (year 2012). The observed mean annual precipitation sum was 1160 mm during the observation. The monthly mean T were mostly positive and slightly negative in winter months, except in 2014 and 2016. The coldest winter period was from

January until March 2013, the warmest from December 2013 until March 2014, while the summer months of 2015 and 2016 were warmer than average. P is distributed evenly over the whole year, partly with very high P sums in the winter and summer months, due to fronts and convective weather phenomena. Heavy precipitation events took place in January 2012, late summer 2014 and in the summer months 2016. During the observation period (2010-2017), snow duration was in average 44 days with a mean snow depth of 13 cm.

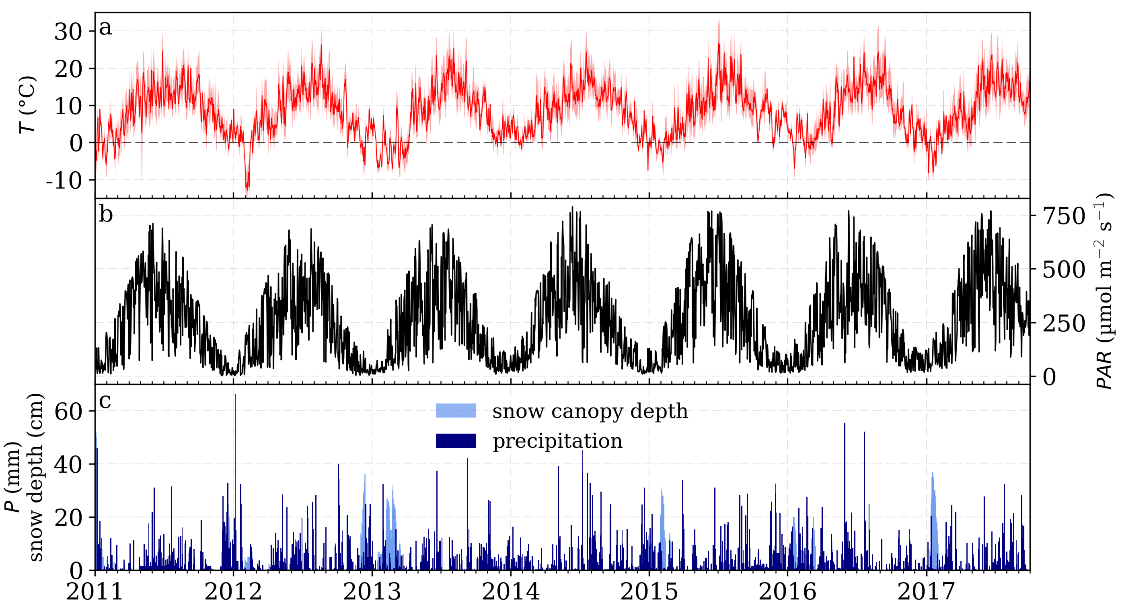

Figure 2: Meteorological overview from 1 January 2011 until 30 September 2017 for the Wüstebach catchment. a) Daily mean air temperature (T). Shaded line marks the daily minimum and maximum values. b) daily means of photosynthetically active radiation (PAR) and c) daily sums of precipitation (P) and daily snow depth. Information about the snow depth were taken from the DWD (German Weather Service) station Kalterherberg (535 m a.s.l.), at a distance of 8.4 km to the study area.

Table 1: Annual means of air temperature (T), photosynthetically active radiation (PAR) and annual sums of precipitation (P) for the years 2011-2016 for the Wüstebach catchment.

year	2011	2012	2013	2014	2015	2016
T (°C)	8.7	7.7	7.1	8.9	8.0	8.5
PAR (µmol m^{-2} s^{-1})	242	224	227	250	269	253
P (mm)	1109	1358	990	1183	1175	1159

3.2 Analyses of flux quality and flux dynamics

After applying quality control in the post processing and u_* filtering analysis to all records of measured NEE, only a total data coverage of 52 % and 60 % remained for the EC station in the forest and deforested area, respectively.

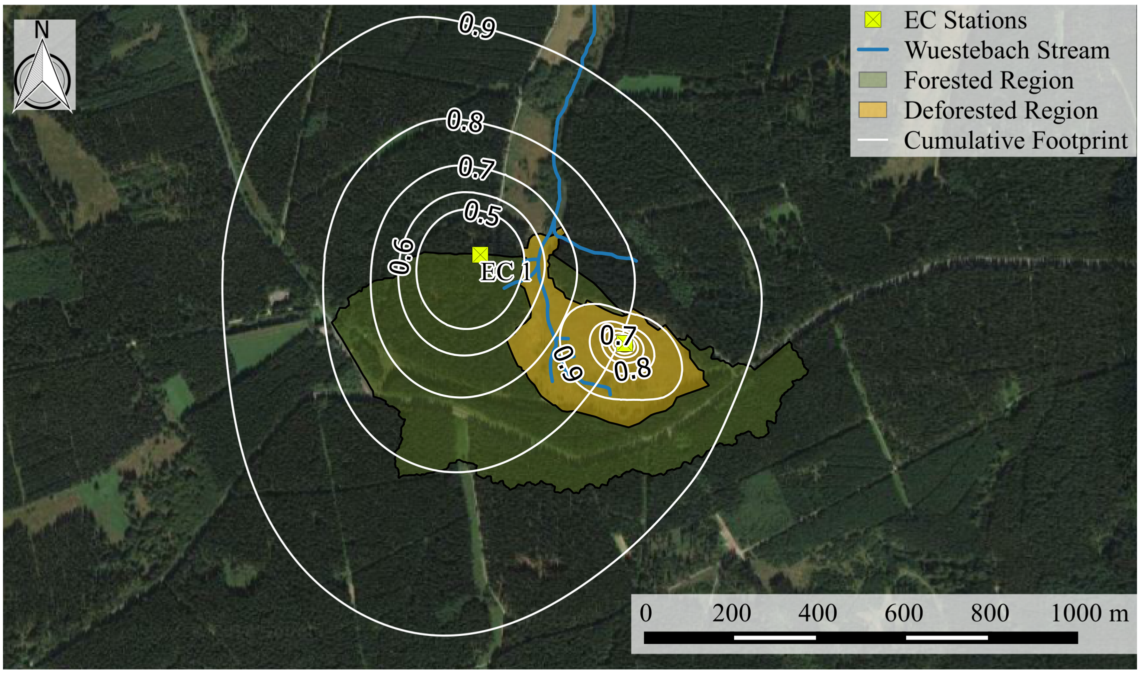

Figure 3: Cumulative footprint analysis for the forest EC station (EC 1) and the EC station at the deforested area. The footprint climatology comprises all evaluable 30-min footprint distribution data of the year 2016. The 0.5, 0.6, 0.7, 0.8 and 0.9 isolines equal 50, 60, 70, 80 and 90 % of source distribution.

The test for energy balance closure on the forest site shows a coefficient of determination (R^2) of 0.85 and an EBR of 85 % (year 2013). The deforested EC-station reached an EBR of 83 % with a R^2 of 0.87 (year 2014 to 2016). An imbalance around 20 % is well known even under otherwise ideal conditions for using the EC method (Wilson et al., 2002).

The footprint analysis in Figure 3 shows that 50 % of the cumulative footprint of the forest EC station originated inside the forested region regardless of the wind direction. The 90 % footprint isoline covered most of the catchment as well as surrounding areas, which consisted mainly of spruce monocultures of the same age and height. With easterly and south-easterly winds, the station was influenced by the deforested area. Therefore, fluxes measured from a wind-direction sector between 63° to 135° were removed in addition to the 70 % criterion described in Section 2.2. This reduced the evaluable EC data for the forest station to 43 %. The extension of the 90 % footprint isoline was approximate 1000 m, which was primarily caused by the height of the measuring tower and measurements during stable stratification (mostly during the night). The footprint of the EC station in the deforested area was much smaller and its shape reflected a channeling effect of the clearcut on the wind direction at this measurement height (2.5 to 3 m a.g.l.). The 90 %-isoline had a maximum extension of 200 m, which is located almost completely within the limits of the deforested area.

As many studies have shown, clearcuts within ecosystems with tall canopies have an impact on wind and turbulence regimes within the atmospheric surface layer (Sogachev et al., 2005; Wang and Davis, 2008; Zhang et al., 2007), as for instance recirculation could lead to downwind on the forest edge, which probably bias EC flux measurements. The size of the recirculation area depends on the height of the overflowed obstacle (Aubinet et al., 2012), here the canopy height (h_c) of the forest. A recirculation area distance of 2 to 5 h_c as formulated in Detto et al. (2008) implies that recirculation may occur within a distance of 50 to 125 m (with h_c = 25 m) between the forest edge and clearcut at our site. This estimated distance did not affect 80 % of the cumulative flux footprint and we assume that the influence of the forest edge on the flux measurements of the clearcut is rather small.

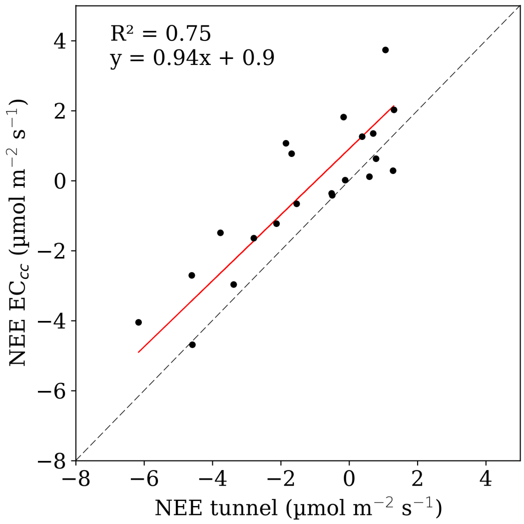

Figure 4: NEE measured with a minimum-disturbance chamber (tunnel) vs. observed NEE from the clearcut EC station. Points represent daily averaged NEE. The red line is the reduced major axis (Webster, 1997). The scattered black line is the 1:1 line.

NEE estimated from roving, manual measurements with a transparent minimum disturbance chamber (end of Sect. 2.4) was compared with those measured by the clearcut EC station (Fig. 4). NEE values sampled during the growing season from April to October 2016 and 2017 were excluded from the analysis in order to preclude an influence of regrowing trees, which were not included in the chamber measurement. According to this criterion and wind speed and direction (Sect. 2.4), 21 out of a total of 34 measurement days remained evaluable. Given the small (1.7 m^2) and changing footprint of the chamber measurements, the regression in Figure 4 shows a fairly good agreement between the chamber and EC measurements with a R^2 of 0.75. This result supports our assumption that recirculation did not largely or systematically affect clearcut EC measurements. During stable conditions, storage fluxes and advection become important, especially for flux measurements over tall canopies and complex terrains. This subject is often discussed as night flux error and is mostly related to an underestimation of CO_2 fluxes during low turbulent conditions which could lead to an underestimation of annual NEE (Aubinet et al., 2000; Goulden et al., 2006; Aubinet et al., 2012). This problem can be solved by discarding affected nighttime data, which is mostly done with an u_* filtering procedure (Aubinet et al., 2012). Since the tower at the forest site is situated on a gentle slope, it is possible that along the topographic gradient cold air drainage flows may occur under stable stratification. Although u* filtering has been applied and resulting gaps were filled, it is possible that annual sums of carbon fluxes might be slightly biased.

3.3 Diurnal, seasonal and interannual changes in carbon fluxes of forest and clearcut before and after deforestation

The open-path self-heating correction (Sec. 2.2) has a negligible small effect on single half-hourly NEE fluxes but gains importance when considering long-term budgets. For this reason and for the sake of clarity, we also show annual totals with this correction in brackets. Figure 5 shows gap-filled half-hourly values of NEE for the forest (top panel) and deforested area (lower panel). Positive values indicate a release from the ecosystem to the atmosphere and negative values the reverse. At the forest site, the maximum amplitude between CO_2 uptake (blue color in the daytime) and release (red color during the night) was higher (40.5 µmol m^{-2} s^{-1}) than in the deforested area (21 µmol m^{-2} s^{-1}). The deforested area was a clear carbon source with positive NEE fluxes in the first year after deforestation. In the following growing seasons, fluxes during the day became increasingly negative caused by regrowth of vegetation.

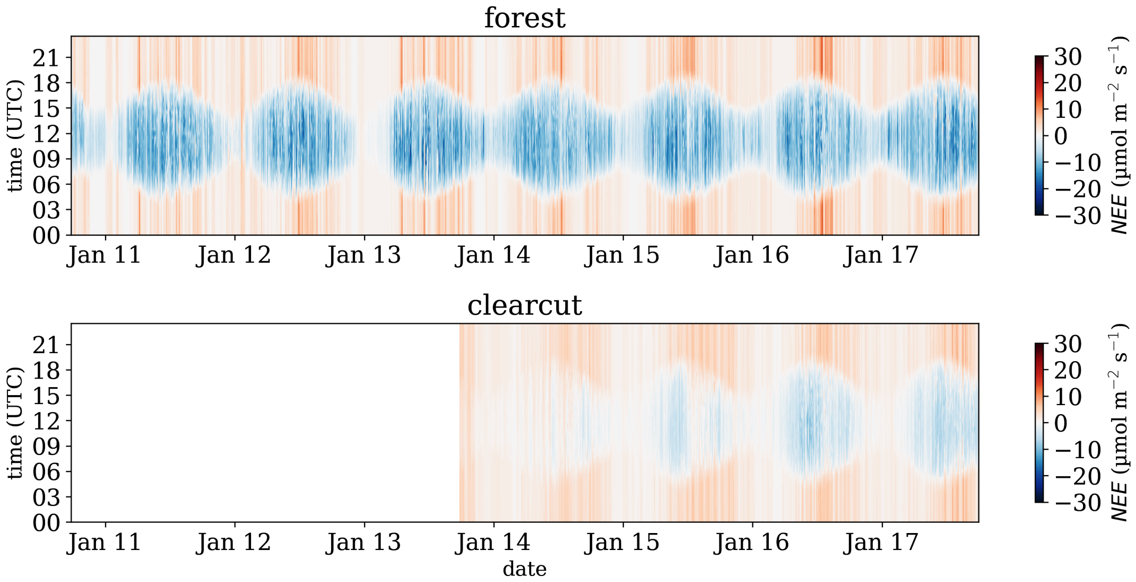

Figure 5: Net ecosystem exchange (NEE) (30-min values, with gap-filling after Lasslop et al., 2010). Top panel shows the values of the forest EC station from 1 October 2010 until 30 September 2017 and the lower panel shows the clearcut from 1 October 2013 until 30 September 2017.

7-day running means for forest NEE fluxes in Figure 6 were mostly negative, even during most of the winter periods, indicating a strong sink for CO_2. Clearcut NEE was mostly positive (0 to 5 µmol m^{-2} s^{-1}) during the first year after the deforestation. In the following years, negative values were reached for short periods during each growing season (-1.0 µmol m^{-2} s^{-1} in 2015 and -2.5 µmol m^{-2} s^{-1} in 2016). Comparing the intra-annual trends of both areas, the period of CO_2 uptake in the forest began earlier and persisted longer than on the clearcut area.

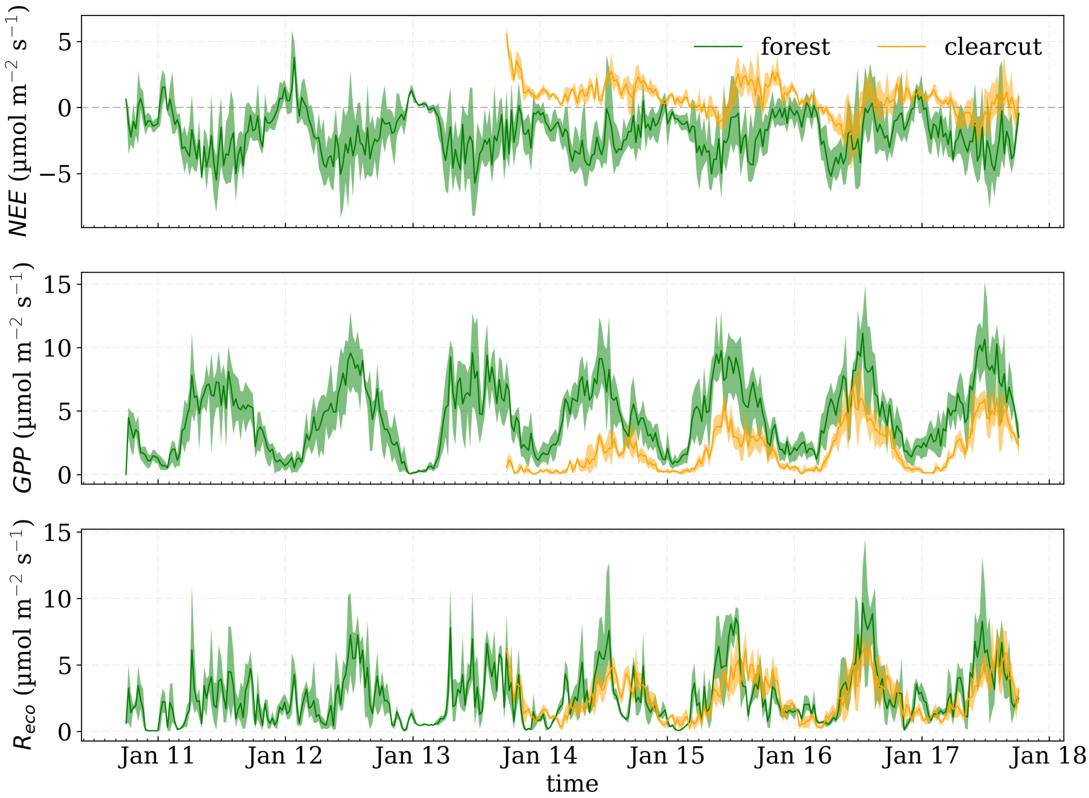

Figure 6: Carbon fluxes of net ecosystem exchange (NEE), gross primary production (GPP) and ecosystem respiration (R_{eco}) as 7-day averages for the forested (green) and de-forested (yellow) area. Shaded areas mark the minima and maxima during the respective 7 days.

During the first year after clear-cutting, strongly reduced photosynthetic uptake is indicated by low fluxes of inferred GPP (2.5 µmol m^{-2} s^{-1}), which approximately tripled in the third year (7.5 µmol m^{-2} $^{-1}$) and remained at this level during the fourth. The level of GPP in the clearcut never exceeded the one in the forest, which ranged in all observed years between 0.5 and 11.0 µmol m^{-2} s^{-1} in winter and summer, respectively. Under sufficient radiation conditions, spruce is still able to assimilate CO_2 even during frost down to -7°C (Schmidt-Vogt, 1989).

7-day averaged fluxes of R_{eco} in the clearcut area were small in the first year (0.5 to 5.0 µmol m^{-2} s^{-1}) and increased slightly until the last year (0.8 to 7.0 µmol m^{-2} s^{-1}). In the first two years after clear-cutting, R_{eco} remained on the same maximum level throughout the seasons and peaked more distinctly in midsummer thereafter, due to proceeding seasonal grass and tree development. The interannual course and amplitude of R_{eco} at the forest site remained relatively stable.

3.4 Annual carbon fluxes of forest and clearcut before and after deforestation

Table 2: Net ecosystem exchange (NEE), gross primary production (GPP) and ecosystem respiration (R_{eco}) from October 2010 for the forested region and from October 2013 for the clearcut until September 2017. Each observation year (y) starts at 1st October. Fluxes determined after correction for self-heating of open-path IRGA (Burba et al., 2008) are declared with *CB*.

Annual total carbon flux forested area							
(g C m^{-2})	y1	y2	y3	y4	y5	y6	y7
NEE	-587	-664	-680	-761	-759	-658	-530
NEE_{CB}	*-481*	*-490*	*-592*	*-594*	*-425*	*-518*	*-648*
GPP	1515	1622	1569	1738	1816	1738	1760
GPP_{CB}	*1496*	*1288*	*1732*	*1980*	*1959*	*1862*	*1966*
R_{eco}	928	958	889	997	1057	1080	1230
$R_{eco,CB}$	*1015*	*798*	*1139*	*1386*	*1533*	*1343*	*1317*
Annual total carbon flux deforested area							
NEE	-	-	-	521	283	95	83
NEE_{CB}	-	-	-	*548*	*374*	*242*	*236*
GPP	-	-	-	385	670	923	892
GPP_{CB}	-	-	-	*447*	*763*	*1062*	*1036*
R_{eco}	-	-	-	906	953	1018	975
$R_{eco,CB}$	-	-	-	*995*	*1137*	*1303*	*1272*

A small interannual variability was observed in the annual sums of NEE, GPP and R_{eco} in the forest (Tab. 2). Throughout the seven-year observation period, the mean annual carbon flux of the forested area was -663±78 (-535±72) g C m^{-2} for NEE, 1680±103 (1755±249) g C m^{-2} for GPP and 1020±106 (1219±232) g C m^{-2} for R_{eco}. These values are comparable with those from long-term observations of a spruce forest in Eastern Germany (Grünwald and Bernhofer, 2007), whereby the uncorrected CO_2 uptake was higher at our study site. Four years after clear-cutting, the deforested area remained a source for CO_2 with a NEE of 83 (236) g C m^{-2}. NEE and GPP changed dynamically in the first three years, followed by a stagnation in the fourth year. While NEE decreased between year 1 and year 2, and GPP increased over the same period, NEE decreased only negligible from the third to the fourth year. At the beginning of the growing period (May and June) 2017, a decline in GPP (Fig. 7) could be observed in analogy to decreased air temperature (Fig. 2), 42 % less *P* and lower mean *PAR* (spring 2016: 361 µmol m^{-2} s^{-1} compared to spring 2017: 322 µmol m^{-2} s^{-1}), which probably have reduced the growth rate of vegetation on the clearcut area. On the contrary, the annual total GPP in the forest, showed an increased sum in 2017 despite the unfavorable weather conditions in spring and early summer. This indicates, that the evergreen spruce forest had a higher resilience towards shifting weather conditions within the vegetation phase than the grass dominated clearcut.

However, stagnation induced by natural fluctuations of the recovery phase of disturbed forest ecosystem is also conceivable. In studies with different types of post-disturbance land management, the shift of NEE from a carbon source to a sink was not linear and showed interannual fluctuations (Humphreys et al., 2005; Lindauer et al., 2014; Aguilos et al., 2014).

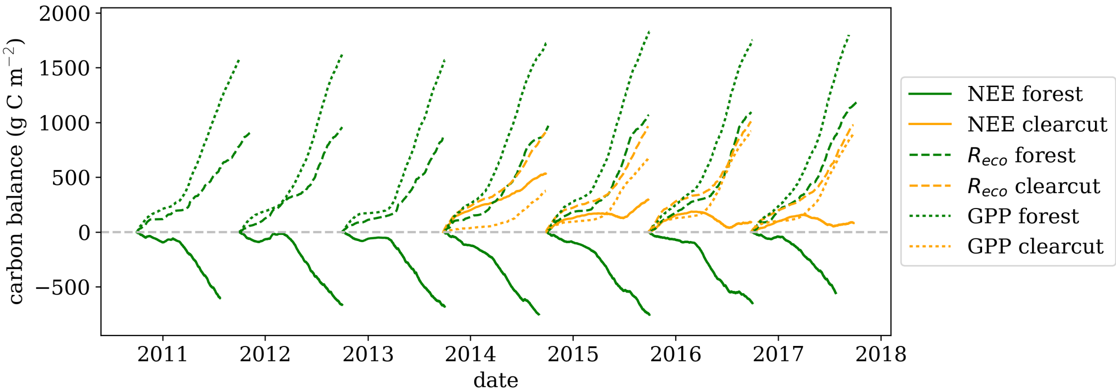

Figure 7: Comparison of the cumulative net ecosystem exchange (NEE), gross primary productivity (GPP) and ecosystem respiration (R_{eco}) in g C m^{-2} (without correction for self-heating of open-path IRGA) from October 2010 for the forested region and October 2013 for the clearcut until September 2017. Each observation year starts at 1st October.

In the clearcut, R_{eco} increased slightly from 906 (995) g C m^{-2} in the first year to 1018 (1303) g C m^{-2} in the third year, which is contrary to observations made in a clearcut with new plantation (Takagi et al., 2009; Paul-Limoges et al., 2015) and a wind-throw disturbed spruce forest (Lindauer et al., 2014), where R_{eco} gained higher values rapidly within the first year of forest succession. In the first years after harvesting, R_{eco} mainly results from wood debris decomposition (Noormets et al., 2012). At our study site, only 3 % of the previous aboveground biomass remained in the field (cf. Section 2.1), which could have suppressed carbon release from decomposition processes. Along with the recovery of the vegetation in the following years, R_{eco} increased simultaneously with increasing GPP. We assume, that above- and below-ground autotrophic respiration act as main contributors to the increase of R_{eco} and decomposition remained comparatively stable. Compared to the forest, the annual total of R_{eco} in the deforested area was lower and always exceeded clearcut GPP.

Compared to changes in evapotranspiration, which was initially reduced by approximately 50 % on the clearcut and returned rapidly towards forest-level values within the first years (Wiekenkamp et al., 2016a), changes in CO_2 fluxes were more profound and long-lasting. After four years, the deforested area still acted as a source for CO_2 on an annual basis, although growing biomass led to a fast increasing uptake through the years.

The ecosystem carbon compensation point, where a regenerating ecosystem changes from source to sink, varies between studies from 3 to 20 years covering a variety of climate conditions, forest ecosystems, stand age and post-disturbance land management (Takagi et al., 2009). Estimations including different chronosequence studies (mainly boreal forests) indicated a compensation point within 20 years after the clear-cutting, with a maximum at 10 years (Aguilos et al., 2014). In a next step, Aguilos et al. (2014) calculated the duration until a forest ecosystem completely recovers all the carbon emitted into the atmosphere after a disturbance. This duration, named payback period, was estimated by dividing the total amount of NEE during the period when the forest was a net source by the annual sum of NEE before disturbances. They concluded that most of the studied sites need at least the same time as they needed to become carbon neutral, and in general more than 20 years to recover all emitted CO_2 (Aguilos et al., 2014).

As can be seen from Tab. 2, the application of self-heating correction adjusted the annual totals towards a larger carbon loss. Reverter et al. (2011) studied the magnitude of this correction using EC data from different ecosystems spanning climate zones from Mediterranean temperate to cool alpine and found that annual corrections of NEE varied between 129 and 190 g C m^{-2} y^{-1}. Thus, they hypothesized that annual carbon balances obtained from measurements using the LI-7500 open-path systems may be biased without applying self-heating correction.

3.5 Albedo effect

Table 3: Annual mean values of albedo (α) for the forest and clearcut site, the difference of the cumulative net ecosystem exchange for forest and clearcut ($\Delta NEE_{f,cc}$ in g C m^{-2}, without correction for self-heating of open-path IRGA), the global radiative forcing of albedo (ΔRF_{α}) and the radiative forcing of CO_2 (ΔRF_{NEE}) in 10^{-14} W m^{-2}(global) m^{-2} (treated surface) and the sum $\sum_{RF}$ of the former for the years after clear-cutting.

	y4	y5	y6	y7
α_{forest}	0.07	0.07	0.07	0.07
$\alpha_{clearcut}$	0.16	0.22	0.25	0.21
$\Delta NEE_{f,cc}$	1282	1042	753	613
ΔRF_{α}	-2.10	-3.56	-4.19	-3.23
ΔRF_{NEE}	0.40	0.73	0.96	1.16
$\sum_{RF}$	-1.70	-2.83	-3.23	-2.08

Whereas the spruce forest showed a mean α of 7 %, α of the deforested area was clearly higher in all study years (Tab. 3). During the first three years after deforestation, α increased from 16 to 25 % presumably due to coverage of initially bare soil surface by grasses and shrubby vegetation. Likewise, the reduction in year 7 could be due to increasing abundance of darker-leaved rowan and broom vegetation (Sect. 2.1). The cooling effect ΔRF_{α} of this higher albedo outweighed the warming effect ΔRF_{NEE} throughout the study period, but due to cumulation of the latter over time, it becomes increasingly important (Rotenberg and Yakir, 2010). As a possible future scenario for the net effect of the study site on global warming, continuing failure to match the high net CO_2 uptake of the adjacent spruce forest throughout the next years, accompanied by a decreasing α as woody vegetation grows on, could turn the present net cooling effect of the deforestation into a warming effect in the medium term. However, α of the eventually expected deciduous natural forest will remain higher than that of spruce forest (various authors after Matthies and Valsta, 2016). Therefore, if ever the cumulative CO_2 sink strength of the new forest compared to spruce reaches a payback point (Aguilos et al., 2014), the point where the net effect of the land cover change is cooling will be reached even earlier due to the albedo effect.

3.6 Comparison of soil respiration and its contribution to ecosystem respiration

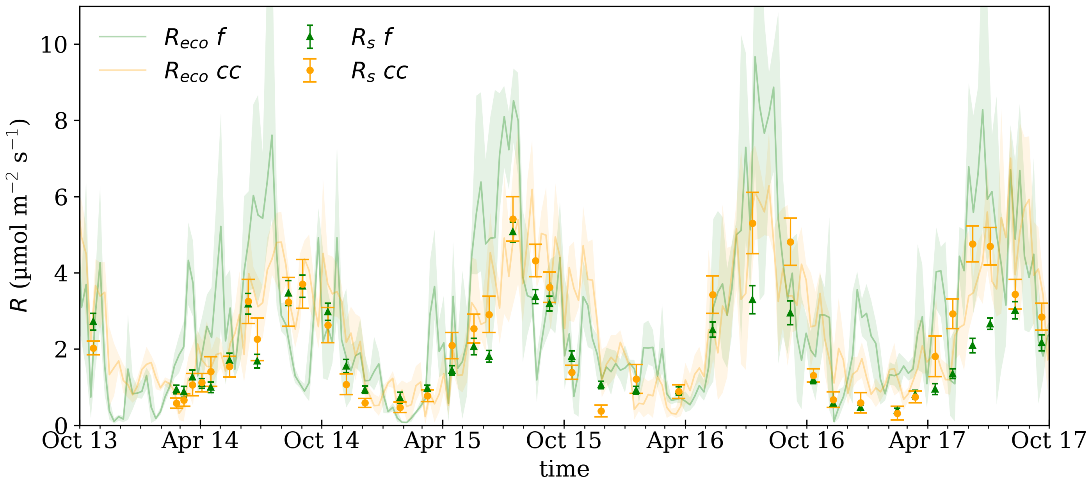

Figure 8: Soil respiration (R_s) averaged over all measurement points for the forest (f) and the clearcut (cc) site. For comparison, total ecosystem respiration (R_{eco}) as also shown in Figure 6. Error bars indicate the 95 % confidence intervals of the mean values of R_s.

R_s of forests accounts for about 30 to 80 % of R_{eco} (Davidson et al., 2006; Acosta et al., 2013) and should therefore be taken into account when studying ecosystem carbon balances. R_s varied in space and time in the forest and deforested area. The area-averaged R_s in forest and clearcut varied monthly and followed a typical seasonal pattern (Fig. 8). In the first year after cutting, maximum respiration rate was reached from late summer to early autumn (forest: 3.6 µmol m^{-2} s^{-1} and clearcut: 3.7 µmol m^{-2} s^{-1}) and the minimum during winter (forest: 0.9 µmol m^{-2} s^{-1}, clearcut: 0.6 µmol m^{-2} s^{-1}). In the following years, R_s peaked in summer (forest: 5.1 µmol m^{-2} s^{-1}, clearcut: 5.4 µmol m^{-2} s^{-1}), while the smallest values were measured in the winter months. The peak in R_s measured in the clearcut increased in the second and third year and stagnated in the last observation year 2017, which is consistent with the observed decreasing R_{eco} in Section 3.4. An increase of R_s in the second and third year after clear-cutting was also observed in a 100-year-old Norway spruce forest, Finland (Kulmala et al., 2014).

In the last two years, the annual range was approximately 1.5 times higher in the clearcut than in the forest. Forest R_s showed approximately the same behavior throughout all observation years for intra-annual minima and maxima. Here, heterotrophic respiration was the dominant component (Fig. 9) during April 2011 until July 2013 with a total average of all measurement points of 59 %, while autotrophic respiration for the various measurement points ranged between 19 and 54 %. These values are consistent with those observed in previous years at the same study site (Dwersteg, 2012). The analysis of one measurement day in March 2014 shortly after deforestation, showed that autotrophic respiration in the clearcut accounted for 16 % of R_s. However, the significance of this single value is limited.

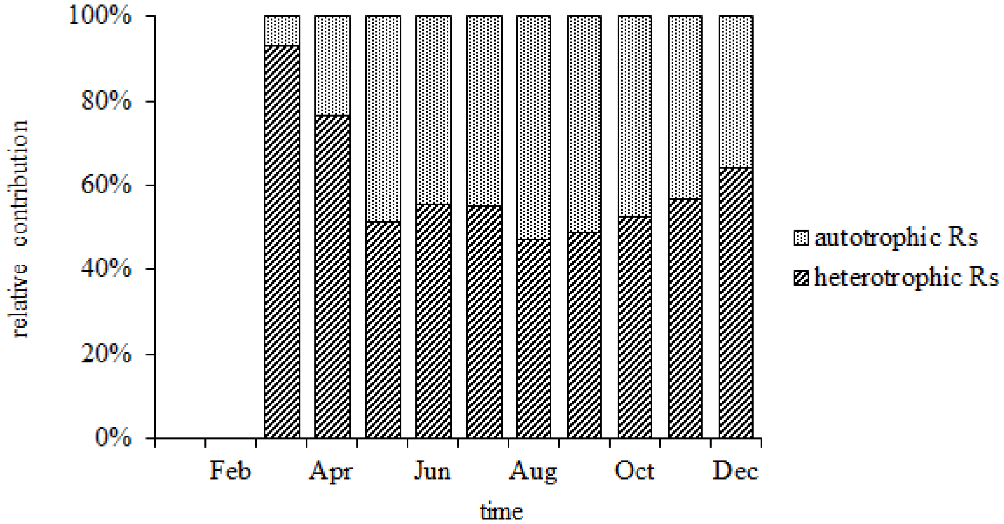

Figure 9: Relative contribution of heterotrophic and autotrophic respiration at the forest site as monthly averages from April 2011 until July 2013. For January and February were no data available.

R_s from both sites followed the seasonal pattern of R_{eco} (Fig. 8), but were less in the forest than in the clearcut, especially during the summer months. The difference of the monthly measured area-averages of R_s between forest and clearcut was not always statistically significant. During winter times and the first two years after cutting, the error bars overlap, indicating no appreciable differences of R_s in the forest and clearcut. In the last two growing seasons, R_s was significantly higher in the clearcut than in the forest, which is probably due to the increased root respiration. Molchanov et al. (2017) studied the effect of clear-cutting on soil CO_2 emission in a spruce forest and reported, that besides soil temperature also the thickness of the litter layer, the degree of damage of the upper soil layer and logging residue on the soil surface have influenced the rate of R_s. They showed that in general R_s was higher in undisturbed soil and plots with litter fall and accumulated logging residues, and was lower in plots with disturbed humus horizons.

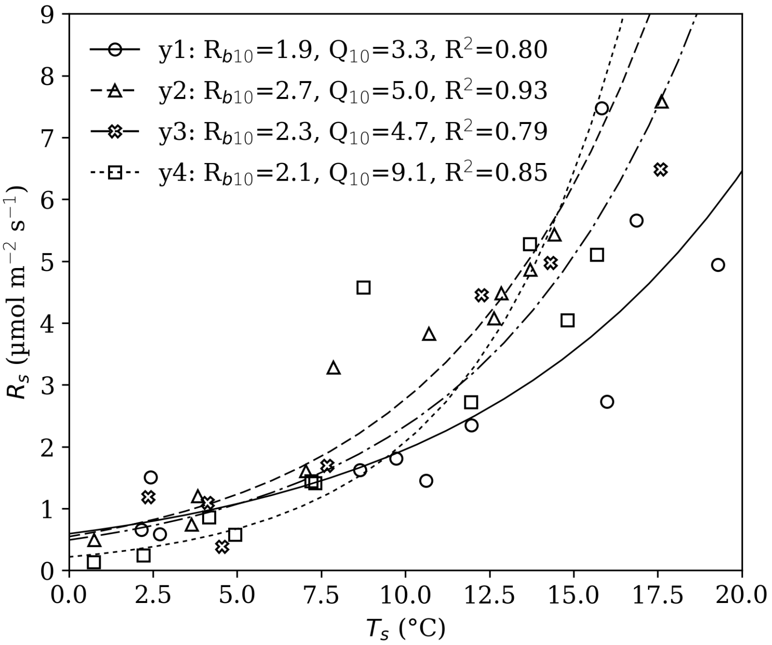

Figure 10: Relationship between monthly soil respiration (R_s) and soil temperature (T_s), both measured next to the clearcut EC station (see Sec2.4 for more information). For each year (y) after deforestation, the base soil respiration at 10°C (R_{sb10}) in , the temperature sensitivity Q_{10} and the R^2 of the regression are given.

At our site, the soil surface was protected against heavy logging machines by padding with spruce branches and the extent of soil damage can be assumed to be relatively small. The relationship between R_s and T_s in the deforested area (Fig.10) was over the entire observation period strong with a R^2 of 0.80, varying between 0.79 and 0.93 in the different years. R_{sb10} was smallest in the first year after deforestation (1.9 µmol m^{-2} s^{-1}) and highest in the second year (2.7 µmol m^{-2} s^{-1}). Afterwards, R_{sb10} decreased to about 2.2 µmol m^{-2} s^{-1}. Q_{10} increased by a factor of 2.7 from the first year after cutting to the last year of observation. We conclude that in the deforested area, temperature and regenerating vegetation played the most important role in controlling temporal patterns of R_s.

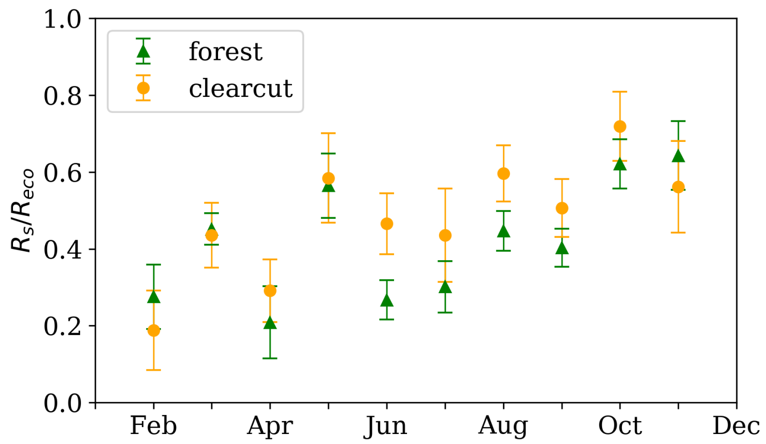

Figure 11: Fraction between monthly soil respiration (R_s) measured by the manual chambers and the corresponding ecosystem respiration (R_{eco}) estimated after Lasslop et al. (2010), calculated as fraction for forest (triangles) and clearcut (circles) and averaged over all observation years after cutting. Error bars indicate the 95 % confidence intervals of the mean values of R_s/R_{eco}. Fractions for January and December were rejected since the evaluable sample size was less than two measurements.

The fraction of R_{eco} originated from R_s was estimated by dividing the spatial average of R_s by R_{eco}, inferred for the respective time stamp from the EC measurements (Section 3.3). Across the year, the clearcut fractions of R_s/R_{eco} in Figure 11 were in general higher (0.5) than for the forest (0.4) due to less above-ground biomass which could respire.

Slightly higher fractions around 0.6 were found for example after harvesting of Douglas-fir forests (Paul-Limoges et al., 2015), which is possibly an indication that autotrophic respiration was more prominent in our clearcut area. The highest R_s/R_{eco} were found in spring and summer months in the deforested area, because of the higher proportion of R_s caused by higher temperatures of the soil surface. In autumn, the forest showed higher fractions, due to the ongoing plant and root activities and possibly dampened and delayed soil cooling. This behavior can also be seen in the comparison of the contributions by heterotrophic and autotrophic respiration to R_s (Fig. 9), where the autotrophic component in autumn is still clearly higher than in the spring months. The trend of R_s/R_{eco} in the forest is comparable with those evaluated for a spruce dominated forest, where the minimum fraction was observed in early spring, followed by increasing values until autumn (Davidson et al., 2006).

4 Summary and Conclusion

We presented seven years of CO_2 flux measurements within a spruce forest catchment in the Eifel National Park, which was partly deforested three years after measurements started and was allowed to regenerate naturally. During the seven years of observation, the spruce forest was a strong sink for CO_2. According to chamber measurements, about 40 % of R_{eco} were due to soil respiration. Within the first year after deforestation, a strong reduction in photosynthetic uptake of CO_2 transformed the clearcut area from a previous sink into a large source for CO_2. In the following years, the annual net CO_2 release from the clearcut decreased continuously, indicating that the area regenerated rapidly. R_s increased continuously year by year and was 1.5 times higher in the last two years than forest R_s. The contribution of R_s to R_{eco} on the clearcut was about 50 %.

The albedo of the clearcut area increased from 0.16 to 0.25 in the third year after cutting and was thus up to 3.5 times higher than the forest albedo. While in the first years anaylzed here, the cooling effect of ΔRF_α outweighs the warming effect ΔRF_{NEE} of the increased NEE release, a decreasing albedo due to a higher proportion of woody vegetation will weaken the cooling effect in the future. Assuming that the albedo of the regenerated deciduous forest remains below that of the spruce forest, however, its effect can be expected to cause an earlier occurrence of compensation and payback points when CO_2 and albedo effects are considered in combination. Existing information about the carbon compensation point and the duration of the payback time (Aguilos et al., 2014) of disturbed forest ecosystems base largely on assumptions made from chronosequence studies or are derived from ecosystem model estimations. With regard to the interaction between land management and climate change, it is important to continue studies such as the one presented here for at least several decades. It has been suggested that the frequency and intensity of natural forest disturbance regimes have increased in the context of climate change (Seidl et al., 2014; Hicke et al., 2012), such that forest management becomes an increasingly important part of climate change mitigation strategies (Canadell and Raupach, 2008; Matthews et al., 2017).

Acknowledgments

This work was supported by the German Federal Ministry of Education and Research (BMBF) in the framework of the project "IDAS-GHG" (FKZ 01LN1313A). Ancillary hardware and its maintenance was supported by TERENO and the DFG Collaborative Research Centre TR32 "Pattern in Soil-Vegetation-Atmosphere Systems". We gratefully thank Nicole Adels, Uwe Baltes and Daniel Dolfus for maintenance ofthe eddy covariance and meteorological measurements.

Appendix

Manual chamber measurements have the advantage that robust spatial averages of soil respiration (R_s) can be estimated with few mobile instruments even for large areas. At the same time, however, they are time-consuming and provide only snapshots in time, typically at a fixed time of the day (late morning to noon in our case). While some of the representativity issues caused by this fact can be solved by relating instantaneous R_s area-averages to simultaneous R_{eco} estimates as in Figure 11, any hypothetical diurnal cycle of this fraction and its effect on conclusions gained from snapshot measurements of R_s will remain unknown. Keane and Ineson (2017) demonstrated for a comparison of R_s between barley and Miscanthus grown on adjacent fields that different diurnal cycles of R_s combined with solely manual measurements at a fixed time-of-day can lead to erroneous conclusions in such comparisons at least in extreme cases.

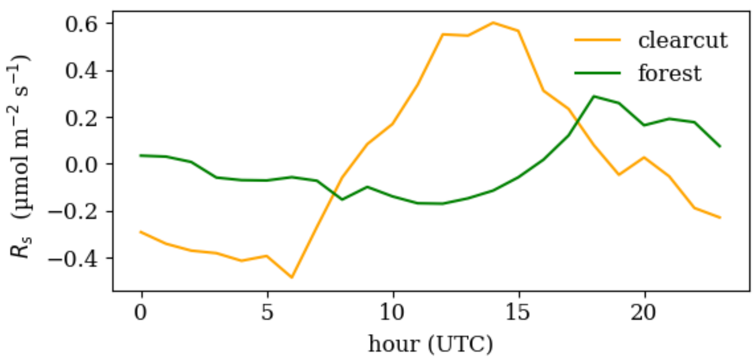

Figure A.1: Site comparison of the normalized mean diurnal cycle of R_s measured with the continuous chamber installation averaged over a period from 8 June until 19 September 2017.

The mean diurnal cycle during the growing season 2017 of R_s is shown in Figure A.1. Diurnal (and annual) cycles in R_s can result from cycles in surface temperature and heat transport into the soil, which act on total respiration via its temperature sensitivity, and from cycles in incoming photosynthetic active radiation, which can influence rhizospheric respiration through assimilate transport (Pavelka et al., 2007; Graf et al., 2008; Kuzyakov and Gavrichkova, 2010; Phillips et al., 2011; Darenova et al., 2014; Zhang et al., 2015). Both transport processes can be subject to similar delay and dampening effects, which may be expected to be larger under a high forest canopy. Consequently, the forest measurement shows a weaker diurnal cycle with a maximum shifted into the evening hours.

Since both curves reflect only a single measurement point in space and their average values (5.0 and 2.5 μ mol m^{-2} s^{-1} for forest and clearcut, respectively) do not reflect the difference between both areas found with area-averaging of the manual measurements (Fig. 8), it remains uncertain whether the differences of up to 0.6 μ mol m^{-2} s^{-1} found in the late morning (Fig. A.1) should be used to correct the manually measured spatial averages. However, it becomes clear from the confidence intervals in Figure 8 that such a correction would not have changed the main finding of clearcut-forest differences that are insignificant during the first two growing seasons after the clearcut and significant during the last two on a 5 % error probability level.

References

Acosta M, Pavelka M, Montagnani L, Kutsch W, Lindroth A, Juszczak R, Janous D (2013) Soil surface CO_2 efflux measurements in Norway spruce forests: Comparison between four different sites across Europe - from boreal to alpine forest. Geoderma 192:295–303, DOI 10.1016/j.geoderma.2012.08.027

Aguilos M, Takagi K, Liang N, Ueyama M, Fukuzawa K, Nomura M, Kishida O, Fukazawa T, Takahashi H, Kotsuka C, Sakai R, Ito K, Watanabe Y, Fujinuma Y, Takahashi Y, Murayama T, Saigusa N, Sasa K (2014) Dynamics of ecosystem carbon balance recovering from a clear-cutting in a cool-temperate forest. Agric For Meteorol 197:26–39, DOI 10.1016/j.agrformet.2014.06.002

Amiro B, Barr A, Black T, Iwashita H, Kljun N, McCaughey J, Morgenstern K, Murayama S, Nesic Z, Orchansky A, Saigusa N (2006) Carbon, energy and water fluxes at mature and disturbed forest sites, Saskatchewan, Canada. Agric For Meteorol 136(3):237–251, DOI 10.1016/j.agrformet.2004.11.012

Amiro BD, Barr AG, Barr J, Black TA, Bracho R, Brown M, Chen J, Clark K, Davis K, Desai A, Dore S, Engel V, Fuentes J, Goldstein A, Goulden M, Kolb T, Lavigne M, Law B, Margolis H, Martin T, McCaughey J, Misson L, Montes-Helu M, Noormets A, Randerson J, Starr G, Xiao J (2010) Ecosystem carbon dioxide fluxes after disturbance in forests of North America. J Geophys Res G: Biogeosci 115(G4), DOI 10.1029/2010JG001390

Aubinet M, Grelle A, Ibrom A, Rannik U, Moncrieff J, Foken T, Kowalski AS, Martin PH, Berbigier P, Bernhofer C, Clement R, Elbers J, Granier A, Gruenwald T, Morgenstern K, Pilegaard K, Rebmann C, Snijders W, Valentini R, Vesala T (2000) Estimates of the annual net carbon and water exchange of forests: The euroflux methodology. Advances in Ecological Research 30:113–175

Aubinet M, Vesala T, Papale D (2012) Eddy covariance: a practical guide to measurement and data analysis. Springer, Dordrecht, 438 pp

Baatz R, Bogena H, Hendricks Franssen H, Huisman J, Montzka C, Vereecken H (2015) An empirical vegetation correction for soil water content quantification using cosmic ray probes. Water Resour Res 51:2030—2046, DOI 10.1002/2014WR016443

Barr A, Richardson A, Hollinger D, Papale D, Arain M, Black T, Bohrer G, Dragoni D, Fischer M, Gu L, Law B, Margolis H, McCaughey J, Munger J, Oechel W, Schaeffer K (2013) Use of change-point detection for friction–velocity threshold evaluation in eddy-covariance studies. Agric For Meteorol 171:31–45, DOI 10.1016/j.agrformet.2012.11.023

Barr AG, Black TA, Hogg EH, Kljun N, Morgenstern K, Nesic Z (2004) Inter-annual variability in the leaf area index of a boreal aspen-hazelnut forest in relation to net ecosystem production. Agric For Meteorol 126(3):237–255, DOI 10.1016/j.agrformet.2004.06.011

Beckers JM, Rixen M (2003) Eof calculations and data filling from incomplete oceanographic datasets. J Atmos Ocean Technol 20(12):1839–1856

Betts R (2000) Offset of the potential carbon sink from boreal forestation by decreases in surface albedo. Nature 408(6809):187–190, DOI 10.1038/35041545

Bogena H, Bol R, Borchard N, Brüggemann N, Diekkrüger B, Drüe C, Groh J, Gottselig N, Huisman JA, Lücke A, Missong A, Neuwirth B, Pütz T, Schmidt M, Stockinger M, Tappe W, Weihermüller L, Wiekenkamp I, Vereecken H (2015) A terrestrial observatory approach for the integrated investigation of the effects of deforestation on water, energy, and matter fluxes. Science China Earth Sciences 58:61–75, DOI 10.1007/s11430-014-4911-7

Bogena HR, Herbst M, Huisman JA, Rosenbaum U, Weuthen A, Vereecken H (2010) Potential of wireless sensor networks for measuring soil water content variability. Vadose Zone Journal 9:1002–1013, DOI 10.2136/vzj2009.0173

Burba GG, McDermitt DK, Grelle A, Anderson DJ, Xu L (2008) Addressing the influence of instrument surface heat exchange on the measurements of CO_2 flux from open-path gas analyzers. Global Change Biology 14(8):1854–1876

Campbell Scientific (2003) HTF3 Soil Heat Flux Plate. Campbell Scientific, Inc., Logan, USA

Canadell JG, Raupach MR (2008) Managing forests for climate change mitigation. Science 320(5882):1456–1457, DOI 10.1126/science.1155458

Clark KL, Gholz HL, Castro MS (2004) Carbon dynamics along a chronosequence of slash pine plantations in north Florida. Ecol Appl 14(4):1154–1171, DOI 10.1890/02-5391

Darenova E, Pavelka M, Acosta M (2014) Diurnal deviations in the relationship between CO_2 efflux and temperature: A case study. Catena 123:263–269, DOI 10.1016/j.catena.2014.08.008

Davidson EA, Richardson AD, Savage KE, Hollinger DY (2006) A distinct seasonal pattern of the ratio of soil respiration to total ecosystem respiration in a spruce-dominated forest. Global Change Biol 12(2):230–239, DOI 10.1111/j.1365-2486.2005.01062.x

Desai AR, Bolstad PV, Cook BD, Davis KJ, Carey EV (2005) Comparing net ecosystem exchange of carbon dioxide between an old-growth and mature forest in the upper Midwest, USA. Agric For Meteorol 128(1):33–55, DOI 10.1016/j.agrformet.2004.09.005

Detto M, Katul GG, Siqueira M, Juang JY, Stoy P (2008) The structure of turbulence near a tall forest edge: The backward-facing step flow analogy revisited. Ecol Appl 18(6):1420–1435, DOI 10.1890/06-0920.1

Dore S, Montes-Helu M, Hart SC, Hungate BA, Koch GW, Moon JB, Finkral AJ, Kolb TE (2012) Recovery of ponderosa pine ecosystem carbon and water fluxes from thinning and stand-replacing fire. Global Change Biol 18(10):3171–3185, DOI 10.1111/j.1365-2486.2012.02775.x

Dwersteg D (2012) Spatial and temporal variability of soil CO_2 efflux in a spruce-dominated forest in the Eifel National Park, Germany. PhD thesis, Rheinischen Friedrich-Wilhelms-Universität Bonn

Erb KH, Kastner T, Plutzar C, Bais ALS, Carvalhais N, Fetzel T, Gingrich S, Haberl H, Lauk C, Iedertscheider MN, Pongratz J, Thurner M, Luyssaert S (2018) Unexpectedly large impact of forest management and grazing on global vegetation biomass. Nature 553(7686):73+, DOI 10.1038/nature25138

Etmann M (2009) Dendrologische Aufnahmen im Wassereinzugsgebiet Oberer Wüstebach anhand Verschiedener Mess- und Schätzverfahren. WWU Münster

Falge E, Baldocchi D, Olson R, Anthoni P, Aubinet M, Bernhofer C, Burba G, Ceulemans R, Clement R, Dolman H, Granier A, Gross P, Grünwald T, Hollinger D, Jensen NO, Katul G, Keronen P, Kowalski A, Lai CT, Law BE, Meyers T, Moncrieff J, Moors E, Munger J, Pilegaard K, Rannik Ü, Rebmann C, Suyker A, Tenhunen J, Tu K, Verma S, Vesala T, Wilson K, Wofsy S (2001) Gap filling strategies for defensible annual sums of net ecosystem exchange. Agric For Meteorol 107(1):43–69, DOI 10.1016/S0168-1923(00)00225-2

Gottselig N, Wiekenkamp I, Weihermüller L, Brüggemann N, Berns A, Bogena H, Borchard N, Klumpp E, Lücke A, Missong A, Pütz T, Vereecken H, Huisman JA, Bol R (2017) A three-dimensional view on soil biogeochemistry: A dataset for a forested headwater catchment. J Environ Qual 46(1):210–218, DOI 10.2134/jeq2016.07.0276

Gough C, Vogel CS, Harrold KH, George K, Curtis PS (2007) The legacy of harvest and fire on ecosystem carbon storage in a north temperate forest. Global Change Biol 13(9):1935–1949, DOI 10.1111/j.1365-2486.2007.01406.x

Goulden ML, Miller SD, Da Rocha HR (2006) Nocturnal cold air drainage and pooling in a tropical forest. J Geophys Res Atmos 111(D8), DOI 10.1029/2005JD006037

Graf A (2017) Gap-filling meteorological variables with Empirical Orthogonal Functions. EGU 2017 General Assembly, Vienna (Austria), 23 Apr 2017 - 28 Apr 2017, URL https://juser.fz-juelich.de/record/829701

Graf A, Weihermüller L, Huisman JA, Herbst M, Bauer J, Vereecken H (2008) Measurement depth effects on the apparent temperature sensitivity of soil respiration in field studies. Biogeosciences 5:1175–1188, DOI 10.5194/bg-5-1175-2008

Graf A, Werner J, Langensiepen M, van de Boer A, Schmidt M, Kupisch M, Vereecken H (2013) Validation of a minimum microclimate disturbance chamber for net ecosystem flux measurements. Agric For Meteorol 174:1–14, DOI 10.1016/j.agrformet.2013.02.001

Graf A, Bogena HR, Drüe C, Hardelauf H, Pütz T, Heinemann G, Vereecken H (2014) Spatiotemporal relations between water budget components and soil water content in a forested tributary catchment. Water Resour Res 50:4837–4857, DOI 10.1016/j.agrformet.2013.02.001

Grant R, Barr A, Black T, Margolis H, McCaughey J, Trofymow J (2010) Net ecosystem productivity of temperate and boreal forests after clearcutting—a Fluxnet-Canada measurement and modelling synthesis. Tellus B 62(5):475–496, DOI 10.1111/j.1600-0889.2010.00500.x

Grünwald T, Bernhofer C (2007) A decade of carbon, water and energy flux measurements of an old spruce forest at the Anchor Station Tharandt. Tellus B 59(3):387–396, DOI 10.1111/j.1600-0889.2007.00259.x

Hicke JA, Allen CD, Desai AR, Dietze MC, Hall RJ, Hogg ETH, Kashian DM, Moore D, Raffa KF, Sturrock RN, Vogelmann J (2012) Effects of biotic disturbances on forest carbon cycling in the United States and Canada. Global Change Biol 18(1):7–34, DOI 10.1111/j.1365-2486.2011.02543.x

van 't Hoff J (1989) Lectures on Theoretical and Physical Chemistry. Part I. Chemical Dynamics (translated by R. A. Lehfeldt). Edwald Arnold, London, pp. 224–229

Hollinger DY, Aber J, Dail B, Davidson EA, Goltz SM, Hughes H, Leclerc MY, Lee JT, Richardson AD, Rodrigues C, Scott NA, Achuatavarier D, Walsh J (2004) Spatial and temporal variability in forest–atmosphere CO_2 exchange. Global Change Biol 10(10):1689–1706, DOI 10.1111/j.1365-2486.2004.00847.x

Humphreys ER, Andrew Black T, Morgenstern K, Li Z, Nesic Z (2005) Net ecosystem production of a Douglas-fir stand for 3 years following clearcut harvesting. Global Change Biol 11(3):450–464, DOI 10.1111/j.1365-2486.2005.00914.x

Humphreys ER, Black TA, Morgenstern K, Cai T, Drewitt GB, Nesic Z, Trofymow JA (2006) Carbon dioxide fluxes in coastal Douglas-fir stands at different stages of development after clearcut harvesting. Agric For Meteorol 140(1):6–22, DOI 10.1016/j.agrformet.2006.03.018

Järvi L, Mammarella I, Eugster W, Ibrom A, Siivola E, Dellwik E, Keronen P, Burba G, Vesala T (2009) Comparison of net CO_2 fluxes measured with open-and closed-path infrared gas analyzers in an urban complex environment. Boreal Environ Res 14:499–514

Keane JB, Ineson P (2017) Technical note: Differences in the diurnal pattern of soil respiration under adjacent Miscanthus giganteus and barley crops reveal potential flaws in accepted sampling strategies. Biogeosciences 14:1181, DOI 10.5194/bg-14-1181-2017

Kittler F, Eugster W, Foken T, Heimann M, Kolle O, Göckede M (2017) High-quality eddy-covariance CO_2 budgets under cold climate conditions. Journal of Geophysical Research: Biogeosciences 122(8):2064–2084, DOI 10.1002/2017JG003830

Knohl A, Kolle O, Minayeva TY, Milyukova IM, Vygodskaya NN, Foken T, Schulze ED (2002) Carbon dioxide exchange of a Russian boreal forest after disturbance by wind throw. Global Change Biol 8(3):231–246, DOI 10.1046/j.1365-2486.2002.00475.x

Kolari P, Pumpanen J, Rannik Ü, Ilvesniemi H, Hari P, Berninger F (2004) Carbon balance of different aged Scots pine forests in Southern Finland. Global Change Biol 10(7):1106–1119, DOI 10.1111/j.1365-2486.2004.00797.x

Kormann R, Meixner FX (2001) An analytical footprint model for non-neutral stratification. Boundary-Layer Meteorol 99:207–224, DOI 10.1023/A:1018991015119

Kowalski AS, Loustau D, Berbigier P, Manca G, Tedeschi V, Borghetti M, Valentini R, Kolari P, Berninger F, Rannik Ü, Hari P, Rayment M, Mencuccini M, Moncrieff J, Grace J (2004) Paired comparisons of carbon exchange between undisturbed and regenerating stands in four managed forests in Europe. Global Change Biol 10(10):1707–1723, DOI 10.1111/j.1365-2486.2004.00846.x

Kowalski S, Sartore M, Burlett R, Berbigier P, Loustau D (2003) The annual carbon budget of a French pine forest (Pinus pinaster) following harvest. Glob Change Biol 9(7):1051–1065, DOI 10.1046/j.1365-2486.2003.00627.x

Kulmala L, Aaltonen H, Berninger F, Kieloaho AJ, Levula J, B/"ack J, Hari P, Kolari P, Korhonen JF, Kulmala M, Nikinmaa E, Pihlatie M, Vesala T, Pumpanen J (2014) Changes in biogeochemistry and carbon fluxes in a boreal forest after the clear-cutting and partial burning of slash. Agric For Meteorol 188:33–44, DOI 10.1016/j.agrformet.2013.12.003

Kuzyakov Y, Gavrichkova O (2010) REVIEW: Time lag between photosynthesis and carbon dioxide efflux from soil: a review of mechanisms and controls. Global Change Biol 16(12):3386–3406, DOI 10.1111/j.1365-2486.2010.02179.x

Lasslop G, Reichstein M, Papale D, Richardson AD, Arneth A, Barr A, Stoy P, Wohlfahrt G (2010) Separation of net ecosystem exchange into assimilation and respiration using a light response curve approach: critical issues and global evaluation. Global Change Biol 16(1):187–208, DOI 10.1111/j.1365-2486.2009.02041.x

Lehmkuhl F, Loibl D, Borchardt H (2010) Geomorphological map of the Wüstebach (Nationalpark Eifel, Germany) - an example of human impact on mid-European mountain areas. J Maps 6:520–530, DOI 10.4113/jom.2010.1118

Lindauer M, Schmid HP, Grote R, Mauder M, Steinbrecher R, Wolpert B (2014) Net ecosystem exchange over a non-cleared wind-throw-disturbed upland spruce forest—Measurements and simulations. Agric For Meteorol 197:219–234, DOI 10.1016/j.agrformet.2014.07.005

Lindroth A, Lagergren F, Grelle A, Klemedtsson L, Langvall O, Weslien P, Tuulik J (2009) Storms can cause Europe-wide reduction in forest carbon sink. Global Change Biol 15(2):346–355, DOI 10.1111/j.1365-2486.2008.01719.x

Liu S, Xu H, Ding J, Chen HYH, Wang J, Xu Z, Ruan H, Chen Y (2016) CO_2 emission increases with damage severity in moso bamboo forests following a winter storm in southern china. Scientific reports 6:30351, DOI 10.1038/srep30351.

Lloyd J, Taylor JA (1994) On the temperature dependence of soil respiration. Functional Ecology pp 315–323

Luyssaert S, Schulze ED, Boerner A, Knohl A, Hessenmoeller D, Law BE, Ciais P, Grace J (2008) Old-growth forests as global carbon sinks. Nature 455(7210):213–215, DOI 10.1038/nature07276

Matthews B, Mayer M, Katzensteiner K, Godbold DL, Schume H (2017) Turbulent energy and carbon dioxide exchange along an early-successional windthrow chronosequence in the European Alps. Agric For Meteorol 232:576–594, DOI 10.1016/j.agrformet.2016.10.011

Matthies BD, Valsta LT (2016) Optimal forest species mixture with carbon storage and albedo effect for climate change mitigation. Ecological Economics 123:95–105, DOI 10.1016/j.ecolecon.2016.01.004

Mauder M, Foken T (2011) Documentation and instruction manual of the eddy-covariance software package TK3, vol 46. University of Bayreuth, Department of Micrometeorology

Mauder M, Cuntz M, Drüe C, Graf A, Rebmann C, Schmid HP, Schmidt M, Steinbrecher R (2013) A strategy for quality and uncertainty assessment of long-term eddy-covariance measurements. Agric For Meteorol 169:122–135, DOI 10.1016/j.agrformet.2012.09.006

Moderow U, Aubinet M, Feigenwinter C, Kolle O, Lindroth A, Mölder M, Montagnani L, Rebmann C, Bernhofer C (2009) Available energy and energy balance closure at four coniferous forest sites across Europe. Theor Appl Climatol 98(3-4):397–412, DOI 10.1007/s00704-009-0175-0

Molchanov AG, Kurbatova YA, Olchev AV (2017) Effect of clear-cutting on soil CO_2 emission. Biology Bulletin 44(2):218–223, DOI 10.1134/S1062359016060121

Myhre G, Highwood EJ, Shine KP, Stordal F (1998) New estimates of radiative forcing due to well mixed greenhouse gases. Geophys Res Lett 25(14):2715–2718, DOI 10.1029/98GL01908

Noormets A, Chen J, Crow TR (2007) Age-dependent changes in ecosystem carbon fluxes in managed forests in northern Wisconsin, USA. Ecosystems 10(2):187–203, DOI 10.1007/s10021-007-9018-y

Noormets A, McNulty SG, Domec JC, Gavazzi G Mand Sun, King JS (2012) The role of harvest residue in rotation cycle carbon balance in loblolly pine plantations. respiration partitioning approach. Global Change Biol 18(10):3186–3201, DOI 10.1111/j.1365-2486.2012.02776.x

Paul-Limoges E, Black T, Christen A, Nesic Z, Jassal R (2015) Effect of clearcut harvesting on the carbon balance of a Douglas-fir forest. Agric For Meteorol 203:30–42, DOI 10.1016/j.agrformet.2014.12.010

Pavelka M, Acosta M, Marek MV, Kutsch W, Janous D (2007) Dependence of the Q10 values on the depth of the soil temperature measuring point. Plant and Soil 292(1-2):171–179, DOI 10.1007/s11104-007-9213-9

Phillips CL, Nickerson N, Risk D, Bond BJ (2011) Interpreting diel hysteresis between soil respiration and temperature. Global Change Biol 17(1):515–527, DOI 10.1111/j.1365-2486.2010.02250.x

Rannik Ü, Altimir N, Raittila J, Suni T, Gaman A, Hussein T, Hölttä T, Lassila H, Latokartano M, Lauri A, Natsheh A, Petäjä T, Sorjamaa R, Ylä-Mella H, Keronen P, Berninger F, Vesala T, Hari P, Kulmala M (2002) Fluxes of carbon dioxide and water vapour over Scots pine forest and clearing. Agric For Meteorol 111(3):187–202, DOI 10.1016/S0168-1923(02)00022-9

REddyProc Team (2014) REddyProc: Data processing and plotting utilities of (half-) hourly eddy-covariance measurements. R package version 1.1.3. URL `https://www.bgc-jena.mpg.de/bgi/index.php/Services/REddyProcWebRPackage`

Reichstein M, Falge E, Baldocchi D, Papale D, Aubinet M, Berbigier P, Bernhofer C, Buchmann N, Gilmanov T, Granier A, Gruenwald T, Havrankova K, Janous D, Knohl A, Laurela T, Lohila A, Loustau D, Matteucci G, Meyers T, Miglietta F, Ourcival JM, Rambal S, Rotenberg E, Sanz M, Tenhunen J, Seufert G, Vaccari F, Vesala T, Yakir D (2005) On the separation of net ecosystem exchange into assimilation and ecosystem respiration: Review and improved algorithm. Global Change Biol 11:1424–1439, DOI 10.1111/j.1365-2486.2005.001002.x

Reverter BR, Carrara A, Fernández A, Gimeno C, Sanz M, Serrano-Ortiz P, Sánchez-Cañete E, Were A, Domingo F, Resco V, Burba G, Kowalski A (2011) Adjustment of annual NEE and ET for the open-path IRGA self-heating correction: Magnitude and approximation over a range of climate. Agricultural and Forest Meteorology 151(12):1856–1861, DOI 10.1016/j.agrformet.2011.06.001

Richardson AD, Hollinger DY (2007) A method to estimate the additional uncertainty in gap-filled NEE resulting from long gaps in the CO_2 flux record. Agric For Meteorol 147(3):199–208, DOI 10.1016/j.agrformet.2007.06.004

Rosenbaum U, Bogena HR, Herbst M, Huisman JA, Peterson TJ, Weuthen A, Western AW, Vereecken H (2012) Seasonal and event dynamics of spatial soil moisture patterns at the small catchment scale. Water Resour Res 48(10), DOI 10.1029/2011WR011518

Rotenberg E, Yakir D (2010) Contribution of semi-arid forests to the climate system. Science 327(5964):451–454, DOI 10.1126/science.1179998

Schmidt-Vogt H (1989) Die Fichte: ein Handbuch in zwei Bänden. Band 2 Krankheiten, Schäden, Fichtensterben. Hamburg, Germany: Parey-Verlag

Seidl R, Rammer W, Jäger D, Lexer MJ (2008) Impact of bark beetle (Ips typographus L.) disturbance on timber production and carbon sequestration in different management strategies under climate change. Forest Ecol Manag 256(3):209–220, DOI 10.1016/j.foreco.2008.04.002

Seidl R, Schelhaas MJ, Rammer W, Verkerk PJ (2014) Increasing forest disturbances in Europe and their impact on carbon storage. Nat Clim Change 4(9):806, DOI 10.1038/nclimate2318

Sogachev A, Leclerc M, Karipot A, Zhang G, Vesala T (2005) Effect of clearcuts on footprints and flux measurements above a forest canopy. Agric For Meteorol 133:182–196, DOI 10.1016/j.agrformet.2005.09.008

Takagi K, Fukuzawa K, Liang N, Kayama M, Nomura M, Hojyo H, Sugata S, Shibata H, Fukazawa T, Takahashi Y, Nakaji T, Oguma H, Mano M, Akibayashi Y, Murayama T, Koike T, Sasa K, Fujinuma Y (2009) Change in CO_2 balance under a series of forestry activities in a cool-temperate mixed forest with dense undergrowth. Global Change Biol 15(5):1275–1288, DOI 10.1111/j.1365-2486.2008.01795.x

Wang W, Davis KJ (2008) A numerical study of the influence of a clearcut on eddy-covariance fluxes of CO_2 measured above a forest. Agric For Meteorol 148(10):1488–1500, DOI 10.1016/j.agrformet.2008.05.009

Wang W, Xiao J, Ollinger SV, Desai AR, Chen J, Noormets A (2014) Quantifying the effects of harvesting on carbon fluxes and stocks in northern temperate forests. Biogeosciences 11(23):6667–6682, DOI 10.5194/bg-11-6667-2014

Webb E (1982) On the correction of flux measurements for effects of heat and water vapour transfer. Boundary Layer Meteorol 23(2):251–254, DOI 10.1002/qj.49710644707

Webster R (1997) Regression and functional relations. Eur J Soil Sci 48:557–566, DOI 10.1111/j.1365-2389.1997.tb00222.x

Wiekenkamp I, Huisman JA, Bogena HR, Graf A, Lin HS, Drüe C, Vereecken H (2016a) Changes in measured spatiotemporal patterns of hydrological response after partial deforestation in a headwater catchment. J Hydrol 542:648–661, DOI 10.1016/j.jhydrol.2016.09.037

Wiekenkamp I, Huisman JA, Bogena HR, Lin HS, Vereecken H (2016b) Spatial and temporal occurrence of preferential flow in a forested headwater catchment. J Hydrol 534:139–149, DOI 10.1016/j.jhydrol.2015.12.050

Wilson K, Goldstein A, Falge E, Aubinet M, Baldocchi D, Berbigier P, Bernhofer C, Ceulemans R, Dolman H, Field C, Grelle A, Ibrom A, Law B, Kowalski T A and; Meyers, Moncrieff J, Monson W Rand Oechel, Tenhunen J, Verma S, Valentini R (2002) Energy balance closure at FLUXNET sites. Agric For Meteorol 113:223–243, DOI 10.1016/S0168-1923(02)00109-0

Wu B, Wiekenkamp I, Sun Y, Fisher AS, Clough R, Gottselig N, Bogena H, Pütz T, Brüggemann N, Vereecken H, Bol R (2017) A dataset for three-dimensional distribution of 39 elements including plant nutrients and other metals and metalloids in the soils of a forested headwater catchment. J Environ Qual 46(6):1510–1518, DOI 10.2134/jeq2017.05.0193

Yamanoi K, Mizoguchi Y, Utsugi H (2015) Effects of a windthrow disturbance on the carbon balance of a broadleaf deciduous forest in Hokkaido, Japan. Biogeosciences 12(23):6837–6851, DOI 10.5194/bg-12-6837-2015

Zacharias S, Bogena H, Samaniego L, Mauder M, Fuß R, Puetz T, Frenzel M, Schwank M, Baessler C, Butterbach-Bahl K, Bens O, Borg E, Brauer A, Dietrich P, Hajnsek I, Helle G, Kiese R, Kunstmann H, Klotz S, Munch JC, Papen H, Priesack W, Schmid HP, Steinbrecher R, Rosenbaum U, Teutsch G, Vereecken H (2011) A network of terrestrial environmental observatories in Germany. Vados Zone Journal 10:955–973, DOI 10.2136/vzj2010.0139

Zhang G, Thomas C, Leclerc MY, Karipot A, Gholz HL, Binford M, Foken T (2007) On the effect of clearcuts on turbulence structure above a forest canopy. Theor Appl Climatol 88(1):133–137, DOI 10.1007/s00704-006-0250-8

Zhang Q, Katul GG, Oren R, Daly E, Manzoni S, Yang D (2015) The hysteresis response of soil CO_2 concentration and soil respiration to soil temperature. J Geophys Res G: Biogeosci 120(8):1605–1618, DOI 10.1002/2015JG003047